Monthly Gridded Data Product of Northern Wetland Methane Emissions Based on Upscaling Eddy Covariance Observations

Olli Peltola[1], Timo Vesala[2,3], Yao Gao[1], Olle Räty[4], Pavel Alekseychik[5], Mika Aurela[1], Bogdan Chojnicki[6], Ankur R. Desai[7], Albertus J. Dolman[8], Eugenie S. Euskirchen[9], Thomas Friborg[10], Mathias Göckede[11], Manuel Helbig[12,13], Elyn Humphreys[14], Robert B. Jackson[15], Georg Jocher[16*], Fortunat Joos[17], Janina Klatt[18], Sara H. Knox[19], Natalia Kowalska[6*], Lars Kutzbach[20], Sebastian Lienert[17], Annalea Lohila[1,2], Ivan Mammarella[2], Daniel F. Nadeau[21], Mats B. Nilsson[16], Walter C. Oechel[22,23], Matthias Peichl[16], Thomas Pypker[24], William Quinton[25], Janne Rinne[26], Torsten Sachs[27], Mateusz Samson[6], Hans Peter Schmid[18], Oliver Sonnentag[13], Christian Wille[27], Donatella Zona[22,28], Tuula Aalto[1]

[1] Climate Research Programme, Finnish Meteorological Institute, P.O. Box 503, 00101 Helsinki, Finland
[2] Institute for Atmosphere and Earth System Research/Physics, PO Box 68, Faculty of Science, FI-00014, University of Helsinki, Finland
[3] Institute for Atmospheric and Earth System Research/Forest Sciences, PO Box 27, Faculty of Agriculture and Forestry, FI-00014, University of Helsinki, Finland
[4] Meteorological Research, Finnish Meteorological Institute, P.O. Box 503, 00101 Helsinki, Finland
[5] Natural Resources Institute Finland (LUKE), FI-00790 Helsinki, Finland
[6] Department of Meteorology, Faculty of Environmental Engineering and Spatial Management, Poznan University of Life Sciences, 60-649 Poznan, Poland
[7] Department of Atmospheric and Oceanic Sciences, University of Wisconsin-Madison, 1225 W Dayton St, Madison, Wisconsin 53706 USA, 608-265-9201, desai@aos.wisc.edu
[8] Department of Earth Sciences, Faculty of Sciences, Vrije Universiteit Amsterdam, Boelelaan 1085, 1081 HV Amsterdam, the Netherlands
[9] University of Alaska Fairbanks, Institute of Arctic Biology, 2140 Koyukuk Dr., Fairbanks, AK 99775
[10] Department of Geosciences and Natural Resource Management, University of Copenhagen , Denmark
[11] Max Planck Institute for Biogeochemistry, Jena, Germany
[12] School of Geography and Earth Sciences, McMaster University, Hamilton, ON, Canada
[13] Département de géographie, Université de Montréal, Montréal, QC H2V 3W8, Canada
[14] Department of Geography & Environmental Studies, Carleton University, Ottawa, ON, Canada
[15] Department of Earth System Science, Woods Institute for the Environment, and Precourt Institute for Energy, Stanford University, Stanford, CA 94305, USA
[16] Department of Forest Ecology and Management, Swedish University of Agricultural Sciences, Umeå, Sweden
[17] Climate and Environmental Physics, Physics Institute and Oeschger Centre for Climate Change Research, University of Bern, Bern, Switzerland
[18] Institute of Meteorology and Climatology – Atmospheric Environmental Research (IMK-IFU), Karlsruhe Institute of Technology (KIT), Kreuzeckbahnstrasse 19, 82467 Garmisch-Partenkirchen, Germany
[19] Department of Geography, The University of British Columbia, Vancouver, Canada
[20] Institute of Soil Science, Center for Earth System Research and Sustainability, Universität Hamburg, Hamburg 20146, Germany
[21] Department of Civil and Water Engineering, Université Laval, Quebec City, Canada
[22] Global Change Research Group, Dept. Biology, San Diego State University, San Diego, CA 92182, USA
[23] Department of Geography, College of Life and Environmental Sciences, University of Exeter, Exeter, EX4 4RJ, UK
[24] Department of Natural Resource Sciences, Thompson Rivers University, Kamloops, BC, Canada

[25] Cold Regions Research Centre, Wilfrid Laurier University, Waterloo, ON, Canada
[26] Department of Physical Geography and Ecosystem Science, Lund University, Lund, Sweden
[27] GFZ German Research Centre for Geosciences, Potsdam, Germany
[28] Department of Animal and Plant Sciences, University of Sheffield, Western Bank, Sheffield, S10 2TN, United Kingdom
*now at: Department of Matter and Energy Fluxes, Global Change Research Institute, Czech Academy of Sciences, Bělidla 986/4a, 603 00 Brno, the Czech Republic

Correspondence to: Olli Peltola (olli.peltola@fmi.fi)

Abstract. Natural wetlands constitute the largest and most uncertain source of methane (CH_4) to the atmosphere, and a large fraction of them are found in the northern latitudes. These emissions are typically estimated using process ('bottom-up') or inversion ('top-down') models. However, estimates from these two types of models are not independent of each other since usually the top-down estimates rely on the a priori estimation of these emissions obtained with process models. Hence, independent, spatially-explicit validation data is needed. Here we utilize a random forest (RF) machine learning technique to upscale CH_4 eddy covariance flux measurements from 25 sites to estimate CH_4 wetland emissions from the northern latitudes (north of 45 °N). Eddy Covariance data from 2005 - 2016 are used for model development. The model is then used to predict emissions during 2013 and 2014.. The predictive performance of the RF model is evaluated using a leave-one-site-out cross-validation scheme. The performance (Nash-Sutcliffe model efficiency = 0.47) is comparable to previous studies upscaling net ecosystem exchange of carbon dioxide and studies comparing process model output against site-level CH_4 emission data. The global distribution of wetlands is one major source of uncertainty for upscaling CH_4. Thus three wetland distribution maps are utilized in the upscaling. Depending on the wetland distribution map, the annual emissions for the northern wetlands yield 32 (22.3-41.2, 95 % confidence interval calculated from a RF model ensemble), 31 (21.4-39.9) or 38 (25.9-49.5) $Tg(CH_4)\ yr^{-1}$. To further evaluate the uncertainties of the upscaled CH_4 flux data products we also compared them against output from two process models (LPX-Bern and WetCHARTs) and methodological issues related to CH_4 flux upscaling are discussed. The monthly upscaled CH_4 flux data products are available at: https://doi.org/10.5281/zenodo.2560163.

1 Introduction

Methane (CH_4) is the second most important anthropogenic greenhouse gas in terms of radiative forcing after carbon dioxide (CO_2): 34 times (GWP_{100}, including climate-carbon feedbacks) as strong as CO_2 (Ciais et al., 2013). CH_4 has contributed ~20% to the cumulative GHG related global warming (Etminan et al. 2016). Deriving constraints on CH_4 sources and sinks is thus of utmost importance. The net atmospheric CH_4 budget is well constrained by precise CH_4 mole fraction measurements around the globe, yet the contribution of individual sources and sinks to this aggregated budget remains poorly understood. This is primarily due to lack of data to constrain the modelling results (Saunois et al., 2016). In order to make more accurate predictions of the atmospheric CH_4 budget in a changing climate, the response of the various sources and sinks to different drivers needs to be better identified and quantified.

Natural wetlands are the largest and quantitatively most uncertain source of CH_4 to the atmosphere (Saunois et al., 2016). An ensemble of land surface models estimated global CH_4 emissions from wetlands for the period 2003-2012 to be 185 Tg(CH_4) yr^{-1} (range 153-227 Tg(CH_4) yr^{-1}) and for the same period inversion models estimated it to be 167 Tg(CH_4) yr^{-1} (range 127-202 Tg(CH_4) yr^{-1}) (Saunois et al., 2016). This discrepancy between bottom-up (process models) and top-down (inversion models) estimates, as well as the range of variability, exemplifies the large uncertainty of the current estimate for natural wetland CH_4 emissions. Sources of this uncertainty can be roughly divided into two categories: 1) uncertainty related to the global areal extent of wetlands (e.g. Petrescu et al 2010. Bloom et al., 2017a; Zhang et al., 2016) and 2) uncertainties related to the key CH_4 emission drivers and responses to these drivers (e.g. Bloom et al., 2017a; Saunois et al., 2017). Evaluation of the emission estimates is thus urgently needed, andresults from these efforts will lead to refined process models. Process model improvements will also directly affect the uncertainty of inversion results since they provide important a priori information to the inversion models (Bergamaschi et al., 2013).

Boreal and arctic wetlands comprise up to 50 % of the total global wetland area (e.g. Lehner and Döll, 2004) and thewetlands in these northern latitudes substantially contribute to total terrestrial wetland CH_4 emissions (ca. 27 %, based on the sum of regional budgets for boreal North America, Europe and Russia in Saunois et al., 2016). In wetlands, CH_4 is produced by methanogenic Archaea under anaerobic conditions and hence the production takes place predominantly under water saturated conditions (e.g. Whalen, 2005). The microbial activity and the resulting CH_4 production is thus controlled by quality and quantity of the available substrates, competing electron acceptors and temperature (Le Mer and Roger, 2001). Once produced, the CH_4 can be emitted to the atmosphere via three pathways: ebullition, molecular diffusion through soil matrix and water column, or plant transport. If plants capable of transporting CH_4 are present, plant transport is generally the dominating emission pathway (Knoblauch et al., 2015; Kwon et al., 2017; Waddington et al., 1996; Whiting and Chanton, 1992). A large fraction of CH_4 transported via molecular diffusion is oxidized into CO_2 by methanotrophic bacteria in the aerobic layers of wetland soils and hence never reaches the atmosphere (Sundh et al., 1995), whereas CH_4 transported via ebullition and plant transport can largely bypass oxidation (Le Mer and Roger, 2001; McEwing et al., 2015). Furthermore, processes related to permafrost (e.g. active layer, thermokarst) and snow cover dynamics (e.g., snow melt, insulation) have an impact on CH_4 flux seasonality and variability (Friborg et al., 1997; Helbig et al., 2017; Mastepanov et al., 2008; Zona et al., 2016; Zhao et al 2016). Hence wetland CH_4 emissions to the atmosphere largely depend on interplay between various controls including water table position, temperature, vegetation composition, methane consumption, availability of substrates and competing electron acceptors.

During the past two decades, eddy covariance (EC) measurements of wetland CH_4 emissions have become more common, due to rapid development in sensor technology (e.g. Detto et al., 2011; Peltola et al., 2013, 2014). The latest generation of low-power and -maintenance instruments are rugged enough for long-term field deployment (Nemitz et al., 2018; McDermitt et al., 2010), thus the number of sites where CH_4 flux measurements have been made is increasing. Due to this progress, EC CH_4 flux synthesis studies have been emerging (Petrescu et al., 2015; Knox et al., in review). Similar progress was made with CO_2

and energy flux measurements in the 1990s and now these measurements form the backbone of the global EC measurement network FLUXNET (https://fluxnet.fluxdata.org/), whose data has provided invaluable insights into terrestrial carbon and water cycles. Some of the most important results have been obtained by upscaling FLUXNET observations using machine learning algorithms to evaluate terrestrial carbon balance components and evapotranspiration (Beer et al., 2010; Bodesheim et al., 2018; Jung et al., 2010, 2011, 2017; Mahecha et al., 2010). These results are now widely used by the modelling community to evaluate process model performance (e.g. Wu et al., 2017) and to validate satellite-derived carbon cycle data products (e.g. Sun et al., 2017; Zhang et al., 2017a).

In this study, we synthesized EC CH_4 flux data from 25 EC CH_4 flux sites and developed an observation-based monthly gridded data product of northern wetland CH_4 emissions. We focus on northern wetlands (north of 45 °N) due to their significance in the global CH_4 budget and relatively good data coverage and process understanding, at least compared to tropical systems (Knox et al., in review). High latitude regions are projected to warm during the next century at a faster rate than any other region, which will likely significantly impact the carbon cycling of wetland ecosystems (Tarnocai, 2009; Zhang et al., 2017b) and permafrost areas of the Arctic-Boreal Region (Schuur et al., 2015). To date, CH_4 emission estimates for northern wetlands are typically based on process models (Bohn et al., 2015; Bloom et al., 2017a; Chen et al., 2015; Melton et al., 2013; Stocker et al., 2013; Wania et al., 2010; Watts et al., 2014; Zhang et al., 2016) or inversion modelling (Bohn et al., 2015; Bruhwiler et al., 2014; Spahni et al., 2011; Thompson et al., 2017; Thonat et al., 2017; Warwick et al., 2016), yet scaling of existing chamber measurements to the northern wetland area has also been published (Zhu et al., 2013). However, CH_4 emission estimates obtained with the former two approaches are not independent since the attribution of CH_4 emissions derived using inversion models to different emission sources (e.g. wetlands) depends largely on *a priori* estimates of these emissions (i.e. process models for wetland emissions), highlighting the tight coupling between these two approaches (Bergamaschi et al., 2013, Spahni et al., 2011). Hence, the main objective of this study is to produce an independent data-driven estimate of northern wetland CH_4 emissions. This product could be used as an additional constraint for the wetland emissions and hence aid in process model refinement and development. Additionally, the drivers causing CH_4 flux variability at the ecosystem scale are also evaluated and methodological issues are discussed which will support future CH_4 wetland flux upscaling studies.

2 Materials and Methods

Data from flux measurement sites (Fig. 1) were acquired and used together with forcing data to estimate CH_4 emissions from northern wetlands with monthly time resolution using a random forest (RF) modelling approach. Both in-situ measurements and remote sensing are utilized in this study. In this section, the RF approach is briefly introduced (Sect. 2.1) and data selection, quality filtering, gap filling and aggregation to monthly values are described (Sect. 2.3). We identified40.7 site-years available for analysis, measured between years 2005 and 2016. To perform upscaling to all wetlands north of 45 °N, gridded data products of the flux drivers and wetland distribution maps were needed. These products are presented in Sect. 2.4 and 2.5,

respectively. Finally, the upscaled wetland CH_4 emissions are compared against process model outputs, with the models briefly described in Sect. 2.6.

Here, wetlands are defined as terrestrial ecosystems with water table positions near the land surface and with plants that have adapted to these water-logged conditions. We exclude lakes, reservoirs and rivers from the study, in addition to ecosystems with significant human influence (e.g. drainage, rewetting). We consider peat forming wetlands (i.e. mires), which can be further classified as fens and bogs based on hydrology, as well as wetlands with hydric mineral soils. Tundra wetlands may have only a shallow peat layer, or none at all. Unified classifications for wetlands are still lacking, and typically different countries follow their own classification scheme, albeit some joint classification schema have been developed (e.g. Ramsar Classification System for Wetland Type).

2.1 Random forest algorithm

Random forest (RF) is a machine-learning algorithm that can be used for classification or regression analyses (Breiman, 2001). In this study the RF models consist of a large ensemble of regression trees. Each individual regression tree is built by training it with a random subset of training data and the trees are trained independently of each other. The RF model output is then the average of all the predictions made by individual regression trees in the forest. Hence the RF algorithm applies the bootstrap aggregation (bagging) algorithm and takes full advantage of the fact that ensemble averaging decreases the noise of the prediction. In addition to random selection of training data, the predictor variables used in split nodes are also selected from a random sample of all predictors which minimizes the possible correlation between trees in the forest (Breiman, 2001) and decreases the possibility of overfitting. The predictor variables can be either categorical or continuous. The variables are then used in the split nodes to divide the data into two (e.g. categorical variable true or false or continuous variable such as e.g. temperature above or below 5 °C).

Performance of RF algorithms to predict CO_2 and energy fluxes across FLUXNET sites have been compared against other machine-learning algorithms such as artificial neural networks and multivariate regression splines by Tramontana et al. (2016) who showed that differences between methods were negligible. We anticipate a similarly negligible effect of machine-learning algorithm choice for CH4 fluxes. For a thorough description of the RF algorithm for flux upscaling purposes, the reader is referred to Bodesheim et al. (2018) (and references therein).

In this study, the RF models were developed using the MATLAB 9.4.0 (R2018a) TreeBagger function with default values similarly to Bodesheim et al. (2018). These settings included a minimum of five samples in a leaf node and used mean squared error (MSE) as a metric for deciding the split criterion in split nodes. Each trained forest consisted of 300 randomized regressions trees.

2.1.1 RF model development for CH_4 flux gapfilling

Our RF algorithm was used for gapfilling the daily CH_4 flux time series The performance of the RF model was evaluated against ‘out-of-bag’ (OOB) data (approximately 1/3 of data for each tree). Since each individual tree in the RF model was

trained using a subset of training data, the rest of the data (i.e. OOB data) can be used as independent validation data to evaluate the prediction performance of that particular regression tree and hence the whole forest (Breiman, 2001). Only the five most important predictors were retained for the gapfilling models for each site. The relative importance of predictors (e.g. air temperature) was evaluated by randomly shuffling the predictor data and then estimating the increase in MSE when model output is compared against OOB data (Breiman, 2001). For important predictors, MSE will increase significantly due to shuffling, whereas the effect of shuffling on MSE is minor for less important predictors. Note that this procedure was executed separately for each site and thus different predictors may have been used for different sites for gapfilling.

2.1.2 RF model development for CH_4 flux upscaling

For upscaling purposes, one RF model was developed using all the available data in order to maximize the information content for the global (>45 °N) CH_4 flux map. The model performance or uncertainty, however, was evaluated using two approaches:. 1) The predictive performance of the model was assessed using the widely used 'leave-one-site-out' cross-validation scheme (e.g. Jung et al., 2011). In order to avoid correlation between training data and validation data, sites located nearby (closer than 100 km) were excluded from the training data (Roberts et al., 2016). 2) The uncertainty of the upscaled fluxes was estimated by bootstrapping. 200 independent RF models were trained using a bootstrap sample of the available data. This yielded 200 predictions for each grid cell and time step in the upscaled CH_4 flux map. The variability over this prediction ensemble was used as an uncertainty measure followinge.g. by Aalto et al. (2018) and Zhu et al. (2013). This uncertainty estimate reflects the ability of the RF model to capture the dependence of CH_4 flux on the used predictors in the available data. However, it does not have any reference to actual in-situ CH_4 fluxes unlike the model predictive performance estimated with cross-validation.

Predictors for the RF model used in the upscaling were determined following Moffat et al. (2010). First, the RF models were trained for each site using one predictor at a time (see all the predictors in Table 1). The single predictor which yielded the best match against validation data (leave-one-site-out scheme) was selected as the primary driver. Then, the RF models were trained again with the primary driver plus each of the other predictors in turn as secondary drivers. Then the RF model performance was again evaluated, and the best predictor pair selected for the next round. This procedure was continued until all the predictors were included in the RF model. The smallest set of predictors capable of producing optimal RF model performance was used for flux upscaling.

2.2 Metrics for model performance evaluation

The RF model performance was evaluated against independent validation data using a set of statistical metrics, which were related to different aspects of model performance. During the RF model training MSE was optimized:

$$MSE = \overline{(o-p)^2}, \quad (1)$$

where o and p are vectors containing the observed and predicted values, respectively, and the overbar denotes averaging.

The Nash-Sutcliffe model efficiency (NSE; Nash and Sutcliffe, 1970) was used to evaluate how well the model was able to predict validation data when compared against a reference (typically the mean of the validation data):

$$NSE = 1 - \frac{\sum_{i=1}^{n}(o_i - p_i)^2}{\sum_{i=1}^{n}(o_i - \bar{o})^2}, \quad (2)$$

where i is index running over all the n values in the o and p vectors. When NSE is equal to 1, there is a perfect match between prediction and observations. Values above 0 imply that the model predicts the observations better than the mean of observations and values below 0 indicate that the predictive capacity of the model is worse than the mean of validation data. Note that NSE calculated with Eq. (2) above is equivalent to the coefficient of determination calculated using residual sum of squares and total sum of squares. However, following the approach used in previous upscaling studies (e.g. Bodesheim et al., 2018; Tramontana et al., 2016), we opted to call this metric NSE. Instead, the coefficient of determination (R^2) was estimated as the squared Pearson correlation coefficient. Note that R^2 and NSE are equal when there is no bias between o and p and the residuals follow Gaussian distribution. Pearson correlation coefficients obtained with different model runs are compared using Fisher's r to z transformation.

The standard deviation (σ) of the model residuals was used to evaluate the spread of model residual values (RE):

$$RE = \sigma(o - p), \quad (3)$$

whereas bias between model predictions and validation data were used to estimate the systematic uncertainty in the upscaled fluxes (BE):

$$BE = \overline{o - p}. \quad (4)$$

Note that RE equals RMSE when there is no systematic difference between the model predictions and observations (i.e. when BE equals zero).

2.3 Data

2.3.1 Data from eddy covariance flux measurement sites

Data were acquired from 25 sites that 1) measure CH_4 fluxes with the EC technique, 2) are located north of 45 °N and 3) are wetlands as defined above and without substantial human influence on ecosystem functioning (see the site locations in Fig. 1 and the site list in Appendix A). The sites were evenly distributed among wetland types: fens (n=9), bogs (7) and wet tundra (9) as well as biomes: tundra (11), boreal (8) and temperate (6), as defined in Olson et al., (2001). At 15 of the 25 sites, sedges (e.g., *Rhynchospora alba, Eriophorum vaginatum, Carex limosa*) were the dominant vascular plant functional type in the flux measurement source area. Most of the sites (18 out of 25) were located north of 60 °N and the highest density of sites were in Fennoscandia and Alaska (Fig. 1). The magnitude of monthly CH_4 flux data varied between sites and the median time series length was 14.5 months of CH_4 flux data per site. Overall, the dataset spanned between years 2005 and 2016. The sites represent northern wetlands sufficiently well to create an upscaled CH_4 flux product based on EC data. Sites are referred to with their FLUXNET IDs and if not available, new temporary site IDs were generated for this study (see Appendix A).

Site PIs provided CH_4 fluxes and their potential drivers (air temperature and pressure, precipitation, wind speed and direction, friction velocity, net ecosystem exchange of CO_2 and its components (canopy photosynthesis and ecosystem respiration), photosynthetically active radiation, water table depth, soil temperature) . However, out of the in-situ measurements only air temperature and precipitation were used for developing the RF model for flux upscaling since gridded data products of the other potentially importantdrivers were not readily available and/or the data for the other drivers were missing from several sites.

Thirty-minute-averaged flux data were acquired from 21 sites and daily data were provided for four sites. The flux time series were quality filtered by removing fluxes with the worst quality flag (based on 0,1,2-flagging scheme, Mauder et al., 2013) and with friction velocity below a site-specific threshold (friction velocity and threshold were available for the site). After filtering, daily medians were calculated if the daily data coverage was above 29 out of 48 half-hourly data points (daily data coverage at minimum 10 data points for sites without diel pattern in CH_4 flux) and no gapfilling was done to the time series prior to calculation of daily values. While this may cause slight systematic bias in the daily flux values, this bias is unlikely to be significant because the magnitude of diel patterns in CH_4 fluxes is typically moderate (e.g. Long et al., 2010) or negligible (e.g. Rinne et al., 2018), although at sites with *Phragmites* cover a relatively strong diurnal cycle can be observed (e.g. Kim et al., 1999; Kowalska et al., 2013).

Unlike the CH_4 flux data, the other in-situ data from the sites were gapfilled prior to the calculation of daily values. The gapfilling was done only if the daily data coverage was above 60 %. or days with lower data coverage, no daily values calculated. Shorter gaps (<2 hours) were filled with linear interpolation, whereas longer gaps (between 2 to 14.5 hours) were replaced with mean diurnal variation within a 30-day moving window. However, for precipitation, daily sums were calculated without any gapfilling. Besides the measurements at the sites, potential solar radiation (R_{pot}) and its time derivative (der(R_{pot})) were calculated based on latitude and time of measurement. In order to remove the R_{pot} latitudinal dependence it was normalized to be between 0 and 1 before usage.

CH_4 flux drivers measured in-situ, in addition to the remote sensing data (Sect. 2.3.2), were used for the gapfilling of CH_4 time series with the RF algorithm (Sect. 2.1.1). For each site the gapfilling models generally agreed well with the independent validation data (mean NSE=0.74 and mean RMSE = 9 nmol m^{-2} s^{-1}). After gapfilling, the CH_4 flux time series were aggregated to monthly values if the monthly data coverage prior to gapfilling was at least 20 %.

The daily time series of air temperature and precipitation measured at the sites were gapfilled using the WATCH Forcing Data methodology applied to ERA-Interim (WFDEI) data (Weedon et al., 2014). Prior to using the WFDEI data for gapfilling, the data were bias corrected for each site as is typically done for climate or weather reanalysis data (e.g. Räisänen & Räty, 2013; Räty et al., 2014). For precipitation, the mean of WFDEI data were simply adjusted to match site mean precipitation. For air temperature the bias correction was done for each month separately using quantile mapping with smoothing within a moving seven-month window. Quantile mapping compares the cumulative distribution functions (CDFs) of WFDEI and site measurements against each other and adjusts the WFDEI data so that after adjustment its CDF matches with the CDF of the

site measurements (e.g. Räisänen & Räty, 2013). After gapfilling the daily time series with WFDEI data, monthly and annual precipitation were calculated, in addition to monthly mean air temperature.

2.3.2 Remote sensing data

Several data products from the Moderate Resolution Imaging Spectrometer (MODIS) were used in this study to derive various driving variables. For RF model development the following data products at 500 m or 1000 m spatial resolution were used: MOD10A1 snow cover (Hall and Rigs, 2016), MOD11A2 daytime and night-time land surface temperature (LSTd and LSTn, Wan et al., 2015), MOD13A3 enhanced vegetation index (EVI, Didan, 2015) and MOD09A1 surface reflectance (Vermote, 2015). More elaborate data products estimating ecosystem gross primary productivity (GPP) and net primary productivity (NPP; MOD17) were not included here for two reasons: 1) many of the sites included here were misclassified in the land cover map used in MOD17 (e.g. as woody savanna), hence severely influencing the estimated GPP and NPP (Zhao et al., 2005), and 2) sites that were correctly classified as permanent wetlands were in fact assigned a fill value and removed from the product since the product is not strictly valid for these areas (Lees et al., 2018). All the remote sensing data products were quality filtered using the quality flags provided along with the data.

The MODIS snow cover ranged from 0 (no snow) to 100 (full snow cover) and was converted to a simple snow cover flag (SC) consisting of 0 and 1 depending whether the snow cover data were below or above 50, respectively. A vector containing days since snow melt (DSSM) was calculated using the snow cover flag and normalized to 0 (beginning) and 1 (end) for each growing season (Mastepanov et al., 2013). The MOD09A1 surface reflectance at bands 2 (841-876 nm) and 5 (1230-1250 nm) were used to calculate the simple ratio water index (SRWI=band 2/band 5) following Zarco-Tejada & Ustin (2001). SRWI showed spurious values when there was snow cover and hence these points were replaced with the mean SRWI observed at each site when there was no snow. Meingast et al. (2014) showed that SRWI can be used as a proxy for wetland water table depth, although their results were affected by changes in vegetation cover, which might hinder across-site comparability in this study. Additionally, following the temperature and greenness modelling approach (Sims et al., 2008), a product of EVI and LSTd was included in the analysis as a proxy for GPP, following a previous peatland study (Schubert et al., 2010). The remote sensing data were provided with daily (MOD10A1), 8-day (MOD09A1, MOD11A2) or monthly (MOD13A3) time resolution and the data were aggregated to monthly means prior to usage.

2.3.3 Additional categorical variables

The sites were also classified based on the presence of permafrost in the source area (present or absent) and according to biome type. Biome types (temperate, boreal, tundra) were determined from Olson et al. (2001) and the information about the permafrost was provided by the site PIs. Furthermore, the data were categorized based on wetland type and sedge cover as in Treat et al. (2018) and Turetsky et al. (2014). However, such information is not available in the gridded format needed for upscaling, nevertheless inclusion of these variables can be used to assess how much they increase the predictive performance of the model.

2.4 Gridded data sets used in flux upscaling

For upscaling CH_4 fluxes using the developed RF model, the LST data were acquired from the aggregated product MOD11C3 (Wan et al., 2015), and snow cover data from MOD10CM (Hall and Riggs, 2018). Distribution of permafrost in the northern latitudes were estimated using the circum-Arctic map of permafrost derived by National Snow and Ice Data Center (Brown et al., 2002). The resolution of the gridded data was adjusted to match the resolution of the wetland maps using bilinear interpolation if needed. Additionally, land and ocean masks (Jet Propulsion Laboratory, 2013) were utilized when processing the gridded data sets.

2.5 Wetland maps

Upscaled fluxes were initially estimated in flux densities per wetland area, that is (amount of CH_4) per (area of wetland) per (unit of time). To create a gridded product of CH_4 emissions from the northern wetlands, these upscaled flux densities were converted into (amount of CH_4) per (grid cell area) per (unit of time) using different wetland maps. Wetland mapping is an ongoing field of research and the usage of different wetland maps contributes to the uncertainty of global wetland CH_4 emission estimates (e.g. Bloom et al., 2017a; Zhang et al., 2017b). Hence, three different wetland maps (PEATMAP, DYPTOP and GLWD) were used in this study to evaluate how much they affect the overall estimates of northern high latitude wetland CH_4 emissions.

The recently developed static wetland map PEATMAP (Xu et al., 2018) combines detailed geospatial information from various sources to produce a global map of wetland extent. Here, the polygons in PEATMAP were converted to fractions of wetland in 0.5° grid cells. While PEATMAP is focused on mapping peatlands, marshes and swamps (typically on mineral soil) are included in the product for certain areas in the northern latitudes. However, most of the wetlands in the northern latitudes are peatlands and thus PEATMAP is suitable for our upscaling purposes. The dynamic wetland map estimated by the DYPTOP model (Stocker et al., 2014) was used by aggregating peat and inundated areas to form one dynamic wetland map with 1° resolution. The widely used Global Lakes and Wetlands Database (GLWD, Lehner and Döll, 2004) is a static wetland map with 30 arc second resolution and since it has been widely used here it provided a point of reference for the other two maps. The map was aggregated to 0.5° resolution and lakes, reservoirs and rivers were excluded from the aggregated map.

2.6 Process models

The upscaled CH_4 fluxes were compared against the output from two process models: LPX-Bern (Spahni et al., 2013; Stocker et al., 2013; Zürcher et al., 2013) and the model ensemble WetCHARTs version 1.0 (Bloom et al., 2017a, 2017b). LPX-Bern is a dynamic global vegetation model which models carbon and nitrogen cycling in terrestrial ecosystems. The model has a separate peatland module with peatland-specific plant functional types (see more details in Spahni et al., 2013). The wetland extent in LPX-Bern was dynamically estimated using the DYPTOP approach with 1° resolution (Stocker et al., 2014). WetCHARTs combines several prescribed wetland maps with different gridded products for heterotrophic respiration and

temperature sensitivity (Q_{10})-parameterizations for CH_4 production to form a model ensemble of wetland CH_4 emissions (Bloom et al., 2017b). Here we used the extended ensemble of WetCHARTs.

3 Results

3.1 Selecting the predictors for the RF model

The predictors in Table 1 were selected one-by-one using the procedure described in Sect. 2.1.2. The order in which the predictors were selected is shown in Fig. 2. LSTn alone gave NSE=0.29. After including the category permafrost presence/absence, R_{pot}, SC and biome class increased NSE to 0.47. However, the influence of SC and biome class on the model performance was marginal based on the small increase in NSE. Additional predictors did not increase the model performance further because 1) they were strongly correlated with a predictor already included in the model (e.g. T_{air} is correlated with LSTn), or 2) the predictors did not contain any information about CH_4 flux variability. The model response to predictors other than biome category was physically reasonable (e.g. permafrost and snow cover decrease fluxes, close to exponential dependence on LSTn), whereas the response to biome category was contrary to expectations. The RF model estimated the CH_4 flux magnitude from the different biomes to be in the order tundra<temperate<boreal, whereas in prior studies it has been shown to be in the order tundra<boreal<temperate (Knox et al., in review; Treat et al., 2018; Turetsky et al., 2014). This discrepancy may be due to the limited number of measurement sites and related sampling bias problems. Hence in order not to upscale an incorrect pattern of decreasing CH_4 emissions when moving from boreal to temperate regions, the biome class was omitted from upscaling. In the subsequent analysis and flux upscaling only the four first predictors (LSTn, permafrost category, R_{pot} and SC) are utilized.

We further tested whether information about wetland type or sedge cover would improve the model performance even though these categorical variables were not available in gridded format and hence were not usable for upscaling. Including the sedge flag increased the NSE to 0.53, although the increase in Pearson correlation was not statistically significant ($p>0.05$, comparison of correlation coefficients using Fisher's r to z transformation). Also, wetland type did not have a statistically significant influence on the model performance ($p>0.05$ and NSE=0.49 if type included). Using too many categorical variables in a RF model may be problematic because each site may end up with a unique combination of categorical variables.

The most important predictor for the model was temperature, similar to numerous studies showing that wetland CH_4 emissions are strongly correlated to soil temperature (Christensen et al., 2003; Helbig et al., 2017; Jackowicz-Korczyński et al., 2010; Rinne et al., 2018; Yvon-Durocher et al., 2014; Knox et al., in review). Selection of LSTn as the primary driver instead of the other temperature variables was likely an outcome of the available data and the used algorithm to select the drivers. With slightly different data set (more sites) other temperature variables (e.g. T_{air}) might have been more important drivers for the CH_4 flux variability. Estimating apparent Q_{10} from the RF model LSTn dependence yielded a value of 1.90+/-0.03 and for validation data it was slightly higher (1.97+/-0.06) (Fig. 3). These values are comparable to the ones reported in Turetsky et al. (2014) for CH_4 chamber measurements at bog and fen sites. The temperature dependence of CH_4 production is modelled in

many process models with the parameter Q_{10} value close to 2 (Xu et al., 2016b), which agrees with the CH_4 emission temperature dependence shown here. However, one should note that also CH_4 oxidation depends on temperature and the derived apparent Q_{10} value describes the temperature dependence of surface CH_4 emission, which is always a combination of CH_4 production and oxidation.

3.2 Model agreement with validation data

The overall systematic bias (BE) between the RF predictions and validation data was negligible (Fig. 4), whereas the spread of the data (RE) was more pronounced (Fig. 4). Following Moffat et al. (2010), RE was analysed further by binning the data based on CH_4 flux magnitude and calculating RE for each bin. RE clearly correlated with flux magnitude (RE = (0.52±0.06)FCH_4+(3.3±2.0) nmol m^{-2} s^{-1}, where FCH_4 denotes CH_4 flux) indicating that the relative random error of the RF model prediction was nearly constant and approximately 50 % for high fluxes. The systematic error BE did not show a clear dependence on flux magnitude. The RF model performance was worse on site mean level than with monthly data. When comparing site means, NSE and R^2 were both 0.25 and RE and BE were 27.0 nmol m^{-2} s^{-1} and 1.5 nmol m^{-2} s^{-1}, respectively. Possible drivers causing the remaining CH_4 flux variability not captured by the RF model (i.e. the scatter in Fig. 4) are discussed in Sect. 4.2.1.

When considering the model performance for each site separately, the agreement shows different characteristics (see Fig. 5 for four examples). For individual sites the magnitude of BE is typically somewhat higher (median of absolute value of BE approximately 11 nmol m^{-2} s^{-1}), whereas RE is lower than for the overall agreement (median RE approximately 10 nmol m^{-2} s^{-1}). These results indicate that the upscaled CH_4 fluxes have in general relatively low bias and high random error, whereas individual pixels in the upscaled CH_4 map may have higher bias, but lower random error.

The mean annual cycle of CH_4 emission predicted by the RF model agrees well with the mean annual cycle calculated from the validation data (not shown). During the nongrowing season the RF model slightly overestimates the fluxes (15 % overestimation) but such differences were negligible during rest of the year the differences are negligible (<1 %). However, for individual sites CH_4 emission seasonality agrees less. For instance, at US-Los the modelled CH_4 emissions start to increase one month earlier in the spring (Fig. 5b). The nongrowing season fluxes are overestimated at four example sites (FI-Sii, US-Los, US-Atq and RU-Ch2; Fig. 5). The mean flux magnitude is modelled well at FI-Sii (Fig. 5a), whereas at US-Los (Fig. 5b) and US-Atq (Fig. 5c) the RF model overestimates and at RU-Ch2 (Fig. 5d) underestimates the CH_4 emissions. The flux bias had a relatively large impact on site-specific NSE. For example, for US-Atq NSE was -1.85, meaning that the observation mean would be a better predictor for this site than the RF model (see the NSE definition in Sect. 2.2). The RF model is not able to replicate the between-year differences in CH_4 emissions at the example sites. Capturing interannual variability has been difficult also in previous upscaling studies of CO_2 and energy fluxes (e.g. Tramontana et al., 2016).

In general, the RF model performance was better for permafrost-free sites than for sites with permafrost ($r = 0.66$ and $r = 0.51$, respectively; $p<0.05$), which is likely related to the fact that at sites with permafrost the MODIS LSTn is not as directly related

to the soil temperature than at sites without permafrost. Hence, LSTn is not as good proxy for the temperature which is controlling both CH_4 production and consumption and this results in a worse performance than at sites without permafrost.

3.3 Upscaled CH_4 fluxes

The RF model developed in this study was used together with the gridded input datasets (Sect. 2.4) and wetland distribution maps (Sect. 2.5) to estimate CH_4 emissions from northern wetlands in 2013 and 2014. The mean CH_4 emissions of the two years from the RF model are plotted in Fig. 6 together with CH_4 wetland emission maps from the process model LPX-Bern and model ensemble WetCHARTs. Differences between the process model estimations and upscaled fluxes are shown in Fig. 7. In general, the spatial patterns are similar among emission maps, which is not surprising given that the spatial variability is largely controlled by the underlying wetland distributions. One noteworthy difference is that WetCHARTs, RF-PEATMAP (i.e. RF modelling with PEATMAP) and RF-GLWD show higher emissions from western Canada than LPX-Bern or the upscaled fluxes using the wetland map from that process model (RF-DYPTOP). The other difference is that RF-GLWD show negligible emissions from Fennoscandia (Fig. 6c). These differences are related to differences in the underlying wetland maps. While the wetland maps differ, there is no consensus on which is more accurate, so comparisons indicate the uncertainty in upscaling emanating from uncertainties in wetland distribution.

Three statistical metrics (NSE, R^2 and RE) were calculated between RF-DYPTOP and LPX-Bern for each grid cell (Fig. 8). The figure illustrates how well the temporal variability of CH4 emissions estimated by RF-DYPTOP and LPX-Bern agree in each grid cell. NSE values are low in areas where the systematic difference between RF-DYPTOP and LPX-Bern was high (compare Figs. 8a and 7a) since the bias strongly penalises NSE. The R^2 values are high throughout the study domain, likely due to the fact that the seasonal cycle of CH_4 emissions dominated the temporal variability in most of the grid cells and the seasonal cycles were in phase between RF-DYPTOP and LPX-Bern. RE values calculated between RF-DYPTOP and LPX-Bern were high in areas where also the emissions estimated by RF-DYPTOP were high (compare Figs. 8c and 6a). This is likely due to the fact that, even though the seasonal cycles were in phase, their amplitudes were different which increased the variability between LPX-Bern and RF-DYPTOP (i.e. increase in RE).

The uncertainties of the upscaled fluxes were estimated from the spread of predictions made with the ensemble of 200 RF models (Fig. 9). The uncertainty mostly scales with the flux magnitude (compare Fig. 6 a)-c) with Fig. 9 a)-c)), meaning that grid cells with high fluxes tend to have also high uncertainties. However, the relative flux uncertainty does have some geographical variation (Fig. 9 d)-f)). The highest relative uncertainties are typically at the highest and lowest latitudes of the study domain. In these locations the dependencies between the predictors and the CH_4 flux are not as well-defined as in the locations with lower uncertainties leading to larger spread in the ensemble of RF model prediction. For instance, at low latitudes LSTn may go beyond the range of LSTn values in the training data (see the range in Fig. 3) and hence the RF model predictions are not well-constrained in these situations. On the other hand, lower relative uncertainties are typically obtained for locations close to the measurement sites incorporated in this study (compare Fig. 1 and 9), since the dependencies between the predictors and the CH_4 flux are better defined.

The seasonalities of the upscaled fluxes and CH_4 fluxes from process models are similar with highest CH_4 emissions in July-August and lowest in February. his seasonal pattern is consistent throughout the study domain (Fig. 10). Warwick et al. (2016) and Thonat et al. (2017) showed that the northern wetland CH_4 emissions should peak in August-September in order to explain correctly the seasonality of atmospheric CH_4 mixing ratios and isotopes measured across the Arctic. Hence the wetland CH_4 emissions presented here are peaking approximately one month too early to perfectly match with their findings. CH_4 flux magnitude agrees well between WetCHARTs and the upscaled flux during spring and midsummer (April-July), whereas LPX-Bern is estimating lower fluxes (0 % and 26 % difference, respectively). During late summer and autumn (August-October) both process models are estimating slightly lower fluxes than the upscaled estimate (17 % and 19 % difference, respectively). The upscaled fluxes show somewhat higher emissions also during the nongrowing season (November-March) than the two process models (27 % and 35 % difference, see Table 2) and the upscaled estimates of nongrowing season emissions are relatively close to a recent model estimate (Treat et al. 2018). This result promotes the recent notion that process models might be underestimating nongrowing season fluxes at high latitudes (e.g. Treat et al., 2018; Xu et al., 2016a; Zona et al., 2016).

Treat et al. (2018) adjusted WetCHARTs model output so that it matches with their estimates of nongrowing season CH_4 emissions and then estimated annual wetland CH_4 emissions north of 40 °N to be 37 ± 7 Tg(CH_4) yr^{-1} using this adjusted model output. The estimates derived here for the annual emissions using the three wetland maps are similar (see Table 2), especially when considering our slightly smaller study domain (above 45 °N). The two process models included in this study estimated slightly lower mean annual emissions than the upscaled fluxes (11 % and 26 % difference between the mean upscaled estimate and WetCHARTs and LPX-Bern, respectively; see also Table 2). However, given the uncertainties in upscaling as well as in process models this can be regarded as relatively good agreement. Different process models may be driven with different climate forcing data and they may have discrepancies in the underlying wetland distributions, in addition to the different parameterisations and descriptions of the processes behind the CH_4 emissions. These sources of uncertainty should be recognised when models are compared against each other or against upscaling products.

In order to further evaluate the agreement between the upscaled fluxes and process models we focused on two specific regions: Hudson Bay Lowlands (HBL) and Western Siberian Lowlands (WSL) (see locations in Fig. 1). The upscaled fluxes indicate higher annual emissions for both subdomains compared to the two process models or previously published estimate (Table 2). For WSL the upscaled estimates are within the range of variability observed between process models and inversion modelling in WETCHIMP-WSL (Bohn et al., 2015) and close to Thompson et al. (2017). The upscaled estimates by Glagolev et al. (2011) might underestimate CH_4 emissions from the WSL area (Bohn et al. ,2015). Furthermore, the process models in Bohn et al. (2015) are likely underestimating the nongrowing season CH_4 emissions which might partly explain the discrepancy to the upscaled estimates in this study. Hence, the upscaled CH_4 emission estimates for the WSL area, while large, are still in a reasonable range.

For HBL, the discrepancy between upscaled emission estimates and the estimates based on process models or previous studies is larger (Table 2). The upscaling results agree with Zhang et al. (2016) and Melton et al. (2013) but show over twice larger emissions from HBL than the other estimates (Table 2). This cannot be explained by wetland mapping since the difference

holds also when DYPTOP wetland map is used in upscaling. There are only few long-term EC flux studies conducted in the HBL area and the only one found (Hanis et al., 2013) showed on average 6.9 g(CH_4) m^{-2} annual emissions at a subarctic fen located in the HBL. If the upscaled CH_4 emissions are downscaled back to ecosystem level at the HBL area with wetland maps, we get on average 11.0 g(CH_4) m^{-2} annual CH_4 emission for the HBL area based on the RF model output, which is 1.6 times larger than the estimate by Hanis et al. (2013). While Hanis et al. (2013) studied only one wetland during different years than here (years 2008-2011 in Hanis et al. (2013), here 2013-2014) it is still noteworthy that the relative difference between Hanis et al. (2013) and this study is similar to the discrepancy between this study and the inversion estimates (Pickett-Heaps et al. (2011); Thompson et al. (2017)) at the whole HBL scale. Pickett-Heaps et al. (2011) and Thompson et al. (2017) show near zero CH_4 emissions during October-April and onset of CH_4 emissions in mid-May or even June, largely dependent on when the ground was free of snow and unfrozen. This is somewhat surprising given the fact that only 32 % of wetlands in the area are underlain by permafrost (based on amalgam of PEATMAP and permafrost map) and hence the soils are likely not completely frozen and some non-growing season CH_4 emissions are likely to occur in such conditions (e.g. Treat et al., 2018). The upscaled nongrowing season CH_4 emissions show on average 1.1 Tg(CH_4) yr^{-1} emissions for the HBL area. This partly, but not completely, explains the discrepancy between the CH_4 emission estimates for the HBL area. All these results suggest that the upscaled product likely overestimates CH_4 emissions from the HBL area.

Discussion

4.1 Comparing the RF model predictive performance to previous studies

The RF model performance was worse when compared against independent validation data than what has been achieved in previous upscaling studies for GPP and energy fluxes (R^2>0.7), and ecosystem respiration (R_{eco}; R^2>0.6) (e.g. Jung et al., 2010; Tramontana et al., 2016). However, the RF model performance for monthly CH_4 emissions was comparable to net ecosystem exchange of CO_2 (NEE) (R^2<0.5) (e.g. Jung et al., 2010; Tramontana et al., 2016). Likely reasons for this finding include for instance that for other fluxes there is simply more data available from several sites spanning the globe. For example, the La Thuile synthesis dataset used by Jung et al. (2010) and Tramontana et al. (2016) consists of 965 site-years of data from over 252 EC stations. Here we have data from 25 sites with CH_4 fluxes. Furthermore, the drivers (or proxies for the drivers) of e.g. GPP and energy fluxes are more easily available from remote sensing (e.g. MODIS) and weather forecasting re-analysis data sets (e.g. WFDEI). In contrast, CH_4 emissions are more related to belowground processes, thus drivers for these processes are more difficult to measure remotely. Also, there are temporal lags between changes in drivers (e.g. LSTn) and CH_4 fluxes in response to these changes. Consequently, training a machine learning model such as RF on such data is difficult since the RF model assumes a instantaneous relationship between the change and response. However, one should also note that GPP or R_{eco} are never directly measured with the EC technique, they are always at least partly derived products (Lasslop et al., 2009; Reichstein et al., 2005). Hence direct functional relationships between GPP and R_{eco} and their environmental drivers are inherently included in these flux estimates, whereas NEE and CH_4 emissions are directly measured without additional

modelling. Also, both NEE and CH_4 emissions are differences between component fluxes(NEE: GPP and R_{eco}; CH_4 flux: production and oxidation). Therefore, GPP and R_{eco} upscaling algorithms show better correspondence with validation data than for NEE or CH_4 emissions and the results for NEE would be the correct point of reference for the RF model performance presented here.

While the RF model performance in this study was inferior to previous upscaling studies for other fluxes when evaluated using different statistical metrics, it was still comparable to what has been shown before for several process models for CH_4 emission (McNorton et al., 2016; Wania et al., 2010; Zürcher et al., 2013; Zhu et al., 2014; Xu et al., 2016a). For instance, McNorton et al. (2016) validated the land-surface model JULES against CH_4 flux data from 13 sites and found R^2=0.10 between the validation data and the model. Wania et al. (2010) found on average RMSE=29 nmol m^{-2} s^{-1} and RMSE=42 nmol m^{-2} s^{-1} with and without tuning their model LPJ-WhyMe against CH_4 flux data from seven sites. Zürcher et al. (2013) found the time-integrated CH_4 flux to be well represented by LPX-Bern model across different sites. A tight correlation (R^2 = 0.92) is found between simulated and measured cumulative site emissions after calibrating the model against the measurements. While Xu et al. (2016a) did not explicitly show any statistical metrics, their model (CLM4.5) comparison against site level CH_4 flux data seemed to be somewhat better than in Wania et al. (2010) or McNorton et al. (2016). Xu et al. (2016a) emphasize the importance of nongrowing season emissions and the fact that their model was clearly underestimating these emissions. Zhu et al. (2014a) calibrated their model (TRIPLEX-GHG) for each measurement site by changing e.g. the Q_{10} for CH_4 production and CH_4 to CO_2 release ratio to be site-specific and found on average R^2=0.64 when comparing the calibrated model against measurements at 17 CH_4 flux measurement sites. However, their findings are not directly comparable to the RF model agreement with validation data shown here due to their model calibration against data before comparison. Nevertheless, their results show that even after calibration, the process models are not fully able to capture the CH_4 flux variability in measurements. Miller et al. (2014) argued that the structure of some of the process models is so complex that the required forcing variables may not be reliable at larger spatial scales. All of these five models (JULES, LPJ-WhyMe, LPX-Bern, CLM4.5 and TRIPLEX-GHG) are contributing to the global CH_4 budget estimation within the Global Methane Project (Saunois et al., 2016), highlighting that these results summarize the agreement between state-of-the-art process models and field measurements.

4.2 Methods to improve RF model predictive performance

4.2.1 Missing predictors

In this study a statistical model was developed using the RF algorithm, and the model was able to yield R^2=0.47 against monthly CH_4 flux validation data. Our upscaling using RF model focused on 2013-2014, as these were the years with the largest overlap of collected data. However, all data from all the years (2005-2016) were used to develop and validate the model. The incomplete match between the RF model and validation data is likely caused by the fact that not all the possible drivers

causing inter- and intra-site variability in CH_4 emissions were included in the analysis and hence all the variability could not be explained by the model.

Christensen et al. (2003) were able to explain practically all the variability (R^2=0.92) in annual CH_4 emissions in their multisite chamber study with only two predictors: temperature and the availability of substrates for CH_4 production. Also, Yvon-Durocher et al. (2014) speculate that the amount of substrates for microbial CH_4 production explains across site variability of CH_4 fluxes in their data. However, gridded data on spatially explicit substrate information n are currently nonexistent. Hence proxies for the substrates available for methanogenesis are needed. The current paradigm on wetland CH_4 emissions is that most of the emitted CH_4 is produced from recently fixed carbon being used as precursors for the CH_4 producing *Archaea* (e.g. Chanton et al., 1995; Whiting and Chanton, 1993). Most process models are based on the premise that a certain fraction of ecosystem net primary productivity (NPP) is available and used for CH_4 production or alternatively a fraction of heterotrophic respiration is allocated to CH_4 emissions (e.g. Xu et al., 2016b). Thus NPP (or GPP) could potentially be included as a predictor for the RF model and used as a proxy for the amount of substrates available for CH_4 production. However, the RF model performance in this study was not enhanced if variables closely related to NPP (EVI and the product of EVI and LSTd) were included as predictors. Also, Knox et al. (in review) did not find GPP as an important predictor of CH_4 emission variability in their multi-site synthesis study.

Using NPP (or proxies for it) for the RF model development might be an oversimplification, since it has been shown that especially the deep-rooting sedges and their NPP are important for CH_4 production (Joabsson and Christensen, 2002; Ström et al., 2003, 2012; Waddington et al., 1996). Hence, information about plant functional types (PFTs) would be needed to better explain the CH_4 flux variability (Davidson et al., 2017; Gray et al., 2013). Furthermore, the fraction of the fixed carbon allocated to the roots and released as root exudates (hence available for CH_4 production) varies between species and root age (Proctor and He, 2017; Ström et al., 2003), further complicating the connection between NPP and CH_4 emissions. The sedges also act as conduits for CH_4 allowing the CH_4 produced below water level to rapidly escape to the atmosphere and bypass the oxic zone in which the CH_4 might have otherwise been oxidized (Waddington et al., 1996; Whiting and Chanton, 1992). Besides sedges, *Spaghnum* mosses are also important because methanotrophic bacteria that live in symbiosis with these mosses significantly decrease the CH_4 emissions to the atmosphere when they are present (Larmola et al., 2010; Liebner et al., 2011; Parmentier et al., 2011; Raghoebarsing et al., 2005; Sundh et al., 1995). In a modelling study, Li et al. (2016) showed that it was essential to consider the vegetation differences between sites when modelling CH_4 emissions from two northern peatlands. Hence, ideally one should have gridded information on wetland species composition and associated NPP across the high latitudes to significantly improve the upscaling results. Unfortunately such information is not yet available and therefore modelled estimates could be used (e.g. LPX-Bern which includes several peatland-specific PFTs allowed to freely evolve during the model run) (Spahni et al., 2013). However, in such case the upscaled CH_4 emission estimates would not be any more model independent and therefore less suitable for model validation. We also note that many process models have only one PFT per wetland.

Different variables related to water input to the ecosystem (i.e. P, P_{ann}) or surface moisture (SRWI) did not enhance the RF model predictive performance, reflecting that water table depth (WTD) is not solely controlled by input of water via precipitation, but also evapotranspiration and lateral flows affect wetland WTD, data that were missing from our study. These findings are consistent with previous studies (e.g. Christensen et al. 2003, Rinne et al. 2018, Pugh et al. 2018 and Knox et al. (in review)) who showed only a modest CH_4 flux dependence on WTD in wetlands/peatlands. In contrast, several chamber-based studies have shown a positive relationship between WTD and CH_4 fluxes (Granberg et al., 1997; Olefeldt et al., 2012; Treat et al., 2018; Turetsky et al., 2014). In general, chamber-based studies often show spatial dependency of CH_4 flux on WTD whereas studies done at ecosystem scale with EC generally do not show temporal WTD dependency, albeit there are exceptions (e.g. Zona et al., 2009). This might indicate that WTD controls meter scale spatial heterogeneity of CH_4 flux between microtopographical features (e.g. Granberg et al., 1997) but not temporal variability on the ecosystem scale, provided that WTD stays relative close to the surface. Also, the chamber studies tend to observe spatial variation, which can be indirectly influenced by WTD via its influence to plant communities, whereas EC studies observe typically temporal variation in sub-annual timescales. However, the effect of WTD might be masked by a confounding effect caused by plant phenology, since vegetation biomass often peaks at the same time as the WTD is at its lowest. While the variables related to WTD did not increase the RF model performance, WTD might still play a role in controlling ecosystem scale CH_4 variability when it is exceptionally high or low. For instance, the year 2006 was exceptionally dry at the Siikaneva fen and hence CH_4 emissions during that year were lower than on average (cf. Fig. 5a). However, in order to accurately capture such dependencies with the machine learning techniques (such as RF), they should be frequent enough so that the model can learn these dependencies.

RF model performance was better at permafrost-free than at permafrost sites which might indicate that the LSTn might not be an appropriate proxy for the temperature controlling the CH_4 production and oxidation rates at sites with permafrost. Also, no information on the development of the seasonally unfrozen, and hydrologically and biogeochemically active layer was included in the RF model. Furthermore, Zona et al. (2016) showed strong hysteresis between soil temperatures and CH_4 emissions at their permafrost sites in Alaska, whereas Rinne et al. (2018) show a synchronous exponential dependence between soil temperature and CH_4 emissions at a boreal fen without permafrost. The hysteresis observed in Zona et al. (2016) could be explained by the fact that part of the produced CH_4 at these permafrost sites is stored belowground for several months before it is being emitted to the atmosphere causing a temporal lag between soil temperature and observed surface flux. In any case, more knowledge on soil processes (soil thawing and freezing, CH_4 production and storage) are needed before the CH_4 emissions from these permafrost ecosystems can be extrapolated to other areas with greater confidence.

It should be emphasized that the drivers causing across site variability in ecosystem scale CH_4 emissions are in general unknown since studies comparing EC CH_4 fluxes from multiple wetland sites have only recently been published (Baldocchi, 2014; Knox et al., in review; Petrescu et al., 2015). Most previous CH_4 synthesis studies were based on plot-scale measurements (Bartlett and Harriss, 1993; Olefeldt et al., 2012; Treat et al., 2018; Turetsky et al., 2014).However, the CH_4 flux responses to environmental drivers and their relative importance might be different at ecosystem scale since CH_4 fluxes typically show significant spatial variability at sub-m scale (e.g. Sachs et al., 2010). Furthermore, the temporal coverage of

plot-scale measurements with chambers is usually relatively poor, whereas EC measurements provide continuous data on ecosystem scale. This study and Knox et al. (in review) show that temperature is important when predicting CH_4 flux variability in a multisite CH_4 flux dataset, but significant fraction of CH_4 flux variability is still left unexplained. It remains a challenge for future EC CH_4 flux synthesis studies to discover the drivers explaining the rest of the variability.

4.2.2 Quality and representativeness of CH_4 flux data

The RF model performance may improve if instrumentation, measurement setup and the data processing are harmonized across sites, since these discrepancies between flux sites might have caused spurious differences in CH_4 fluxes. These differences would have created additional variability in the synthesis dataset which would in turn 1) influence the training of RF model and 2) decrease e.g. NSE values obtained against validation data since there would be artificial variability in the validation data which is not related to the predictors. In this study, the site PIs processed the data themselves using different processing codes, albeit the gapfilling was done centrally in a standardized way.

While these issues mentioned above could impact the upscaling results shown here, prior studies have shown that the usage of different instruments or processing codes do not significantly impact CH_4 flux estimates. For instance, Mammarella et al. (2016) showed that the usage of different processing codes (EddyPro and EddyUH) resulted in general in 1 % difference in long-term CH_4 emissions. On the other hand, CH_4 instrument cross comparisons have shown small differences (typically less than 7 %) between the long term CH_4 emission estimates derived using different instruments (Goodrich et al., 2016; Peltola et al., 2013, 2014). While these studies show consistent CH_4 emissions they also stress that the data should be carefully processed to achieve such good agreement across processing codes and instruments. In addition, many issues related to e.g. friction velocity filtering and gapfilling of CH_4 fluxes are still unresolved, and the role of short-term emission bursts, which are common in methane flux time series, needs to be further investigated (e.g. Schaller et al., 2017). However, recently Nemitz et al. (2018) advanced these issues by proposing a methodological protocol for EC measurements of CH_4 fluxes used to standardize CH_4 flux measurements within the ICOS measurement network (Franz et al, 2018).

Twenty-five flux measurement sites were included in this study and they were distributed across the Arctic-Boreal region (see Fig. 1). The measurements were largely concentrated in Fennoscandia and Alaska, whereas data from e.g. the HBL and WSL areas were missing. Long-term EC CH_4 flux measurements are largely missing from these vast wetland areas casting uncertainty on wetland CH_4 emissions from these areas. The location of a flux site is typically restricted by practical limitations related to e.g. ease of access and availability of grid power. Hence open-path instruments with low power requirements potentially open up new areas for flux measurements (McDermitt et al., 2010), yet they need continuous maintenance which is not necessarily easy in remote locations. However, one could argue that the geographical location of flux sites is not vital for upscaling, more important is that the available data represents well the full range of CH_4 fluxes across the northern latitudes and more importantly the CH_4 flux responses to the environmental drivers. Also, sites should ideally cover all different wetlands with varying plant species composition, whereas geographical representation is not necessarily as important. CH_4 flux site representativeness could be potentially assessed in the same vein as in previous studies for other measurement

networks (Hargrove et al., 2003; Hoffman et al., 2013; Papale et al., 2015; Sulkava et al., 2011). However, before such analysis can be done, the main drivers causing across sites variability in ecosystem scale CH_4 fluxes should be better identified.

Most of the CH_4 flux data here and in the literature have been recorded during the growing season when the CH_4 fluxes are at maximum, whereas year-round continuous CH_4 flux measurements are not as common. This is likely due to the harsh conditions in the Arctic during winter which make continuous high-quality flux measurements very demanding (e.g. Goodrich et al., 2016; Kittler et al., 2017a), but also in part since the large-scale importance of nongrowing season emissions has just recently been recognized (Kittler et al., 2017b; Treat et al., 2018; Xu et al., 2016a; Zona et al., 2016). For upscaling year-round CH_4 emissions, continuous measurements are vital to accurately constrain also the non-growing season emissions and their drivers.

5 Data availability

The presented upscaled CH_4 flux maps (RF-DYPTOP, RF-PEATMAP and RF-GLWD), their uncertainties and the underlying CH_4 flux densities are accessible via an open-data repository Zenodo (Peltola et al., 2019). The datasets are saved in netCDF-files and they are accompanied by a readme file. The dataset can be downloaded from https://doi.org/10.5281/zenodo.2560163.

6 Conclusions

Methane (CH_4) emission data comprising over 40 site-years from 25 eddy covariance flux measurement sites across the Arctic-Boreal region were assembled and upscaled to estimate CH_4 emissions from northern (>45 °N) wetlands. The upscaling was done using the random forest (RF) algorithm. The performance of the RF model was evaluated against independent validation data utilizing the leave-one-site-out scheme which yielded value of 0.47 for both the Nash-Sutcliffe model efficiency and R^2. These results are similar to previous upscaling studies for the net ecosystem exchange of carbon dioxide (NEE) but are less good than for the individual components of NEE or energy fluxes (e.g. Jung et al., 2010; Tramontana et al., 2016). The performance is also comparable to studies where process models are compared against site CH_4 flux measurements (McNorton et al., 2016; Wania et al., 2010; Zürcher et al., 2013; Zhu et al., 2014; Xu et al., 2016a). Hence, despite the relatively high fraction of unexplained variability in the CH_4 flux data, the upscaling results are useful for comparing against models and could be used to evaluate model results. The three gridded CH_4 wetland flux estimates and their uncertainties are openly available for further usage (Peltola et al., 2019).

The upscaling to the regions > 45 °N resulted in mean annual CH_4 emissions comparable to prior studies on wetland CH_4 emissions from these areas (Bruhwiler et al., 2014; Chen et al., 2015; Spahni et al., 2011; Treat et al., 2018; Watts et al., 2014; Zhang et al., 2016; Zhu et al., 2013) and hence in general support the prior modelling results for the northern wetland CH_4 emissions. When compared to two validation areas, the upscaling likely overestimated CH_4 emissions from the Hudson Bay Lowlands, whereas emission estimates for the western Siberian lowlands were in a reasonable range. Future CH_4 flux upscaling

studies would benefit from long-term continuous CH_4 flux measurements, centralized data processing and better incorporation of CH_4 flux drivers (e.g. wetland vegetation composition and carbon cycle) from remote sensing data needed for scaling the fluxes from the site level to the whole Arctic-boreal region.

Appendix A

Table A1. Description of eddy covariance sites included in this study.

Time resolution of data	Wetland type	Biome based on Olson et al. (2011)	permafrost present (true/false)	sedges as dominant vegetation type (true/false)	Reference	Amount of monthly CH_4 flux data available	Latitude, Longitude	Site PI	Site ID	Name
30 min	bog	temperate	false	false	Hommeltenberg et al. (2014)	2	47.8064, 11.3275	Janina Klatt, Hans Peter Schmid	DE-SfN	Schechenfilz Nord
30 min	wet tundra	tundra	true	true	Parmentier et al. (2011)	5	70.8291, 147.4943	Albertus J. Dolman	RU-Cok	Chokurdakh
30 min	wet tundra	tundra	true	false	Maruschak et al. (2016)	5	67.0547, 62.9405	Thomas Friborg	RU-Vor	Vorkuta
30 min	fen	tundra	false	true	Jammet et al. (2017)	6	68.3542, 19.0503	Thomas Friborg	SE-St1	Stordalen
30 min	bog	tundra	true and false[a]	false		55	68.3560, 19.0452	Janne Rinne	SE-Sto	Stordalen (ICOS)*

30 min	fen	boreal	false	true	Rinne et al. (2018)	104	61.8327, 24.1928	Timo Vesala, Ivan Mammarella	FI-Sii	Siikaneva 1
30 min	bog	boreal	false	false	Korrensalo et al. (2018)	26	61.8375, 24.1699	Timo Vesala, Ivan Mammarella	FI-Si2	Siikaneva 2
30 min	fen	boreal	false	true	Aurela et al. (2009)	59	67.9972, 24.2092	Annalea Lohila	FI-Lom	Lompolojänkkä
daily	bog	boreal	false	false	Nadeau et al. (2013)	3	53.6744, -78.1706	Daniel F. Nadeau	CA-JBL	James Bay lowlands
30 min	fen	temperate	false	false	Pugh et al. (2018)	30	46.0827, -89.9792	Ankur R. Desai	US-Los	Lost Creek
30 min	wet tundra	tundra	true	true	Zona et al. (2016)	11	70.4696, -157.4089	Donatella Zona	US-Atq	Atqasuk
30 min	wet tundra	tundra	true	true	Zona et al. (2016)	16	71.2810, -156.6123	Donatella Zona	US-Beo	Barrow Environmental Observatory
30 min	wet tundra	tundra	true	true	Zona et al. (2016)	16	71.2809, -156.5965	Donatella Zona	US-Bes	Biocomplexity Experiment

										South tower
30 min	wet tundra	tundra	true	true	Zona et al. (2016)	15	68.4865, -155.7502	Donatella Zona	US-Ivo	Ivotuk
30 min	fen	temperate	false	false	Long et al. (2010)	5	54.9538, -112.4670	Lawrence B. Flanagan	CA-WP1	Western peatland 1
daily	bog	temperate	false	false	Brown et al. (2014)	16	45.4094, -75.5186	Elyn Humphreys	CA-Mer	Mer Bleue
daily	wet tundra	boreal	true	true	Kittler et al. (2017)	21	68.6169, 161.3509	Mathias Göckede	RU-Ch2	Chersky reference
30 min	fen	temperate	false	true	Kowalska et al. (2013)	4	52.7622, 16.3094	Bogdan Chojnicki	PL-wet	Rzecin
30 min	fen	boreal	false	true	Nilsson et al. (2008)	22	64.1820, 19.5567	Mats B. Nilsson, Matthias Peichl	SE-Deg	Degerö Stormyr
daily	fen	temperate	false	true	Pypker et al. (2013)	5	46.3167, -86.0500	Thomas Pypker	US-Sen	Seney

30 min	bog	boreal	false	false	Helbig et al. (2016)	14	61.3000, -121.3000	Oliver Sonnentag	CA-SCC	Scotty Creek
30 min	wet tundra	tundra	true	true	Sachs et al. (2008)	11	72.3667, 126.5000	Torsten Sachs	RU-Sam	Samoylov
30 min	wet tundra	tundra	true	true		7	68.6060, -149.3110	Eugenie S. Euskirchen	US-ICh	Imnavait Creek
30 min	fen	boreal	false	true	Euskirchen et al. (2014)	16	64.7040, -1483130	Eugenie S. Euskirchen	US-BCF	Bonanza Creek, fen
30 min	bog	boreal	false	false	Euskirchen et al. (2014)	14	64.7000, -148.3200	Eugenie S. Euskirchen	US-BCB	Bonanza Creek, bog

[a] Data from this site is divided into two since data from two wind directions differ from each other (with and without permafrost).

Author contribution

OP, TA and TV designed the study and YG contributed further ideas for the study. OP did the data processing and analysis, except OR prepared the PEATMAP map for the study. PA, MA, BC, ARD, AJD, ESE, TF, MG, MH, EH, GJ, JK, NK, LK, AL, IM, DFN, MBN, WCO, MP, TP, WQ, JR, TS, MS, HPS, OS, CW and DZ provided CH_4 fluxes and other in-situ data for the study. FJ and SL did the LPX-Bern model runs. OP wrote the first version of the manuscript and all authors provided input.

Competing interests

The authors declare that they have no conflict of interest.

Acknowledgments

Lawrence B. Flanagan is acknowledged for providing data from CA-WP1 site. Lawrence B. Flanagan acknowledge support from the Natural Sciences and Engineering Council of Canada and Canadian Foundation for Climate and Atmospheric Sciences. OP is supported by the Postdoctoral Researcher project (decision 315424) funded by the Academy of Finland. OR is supported by the Academy of Finland IIDA-MARI project (decision 313828). The financial support by the Academy of Finland Centre of Excellence (272041 and 307331), Academy Professor projects (312571 and 282842), ICOS-Finland (281255), CARB-ARC project (285630) are acknowledged. SHK and RBJ acknowledge support from the Gordon and Betty Moore Foundation through Grant GBMF5439 'Advancing Understanding of the Global Methane Cycle'. ARD acknowledges support of the DOE Ameriflux Network Management Project. AJD acknowledges support from the Netherlands Earth System Science Centre, NESSC). TS was supported by the Helmholtz Association of German Research Centres (grant VH-NG-821). IM and TV thank the EU for supporting the RINGO project funded by the Horizon 2020 Research and Innovation Programme (grant agreement 730944). Also EU-H2020 CRESCENDO project (641816) is acknowledged. FJ and SL thank for support by the Swiss National Science Foundation (#200020_172476). MBN and MP acknowledge support from the National Research Council (VR, 2018-03966) SITES and ICOS-Sweden.

References

Aalto, J., Karjalainen, O., Hjort, J. and Luoto, M.: Statistical Forecasting of Current and Future Circum-Arctic Ground Temperatures and Active Layer Thickness, Geophys. Res. Lett., 45(10), 4889–4898, doi:10.1029/2018GL078007, 2018.

Aurela, M., Lohila, A., Tuovinen, J.-P., Hatakka, J., Riutta, T. and Laurila, T.: Carbon dioxide exchange on a northern boreal fen, BOREAL Environ. Res., 14(4), 699–710, 2009.

Baldocchi, D.: Measuring fluxes of trace gases and energy between ecosystems and the atmosphere – the state and future of the eddy covariance method, Glob. Chang. Biol., 20(12), 3600–3609, doi:10.1111/gcb.12649, 2014.

Bartlett, K. B. and Harriss, R. C.: Review and assessment of methane emissions from wetlands, Chemosphere, 26(1), 261–320, doi:https://doi.org/10.1016/0045-6535(93)90427-7, 1993.

Beer, C., Reichstein, M., Tomelleri, E., Ciais, P., Jung, M., Carvalhais, N., Rödenbeck, C., Arain, M. A., Baldocchi, D., Bonan, G. B., Bondeau, A., Cescatti, A., Lasslop, G., Lindroth, A., Lomas, M., Luyssaert, S., Margolis, H., Oleson, K. W., Roupsard, O., Veenendaal, E., Viovy, N., Williams, C., Woodward, F. I. and Papale, D.: Terrestrial Gross Carbon Dioxide Uptake: Global Distribution and Covariation with Climate, Science (80-.)., 329(5993), 834–838, doi:10.1126/science.1184984, 2010.

Bergamaschi, P., Houweling, S., Segers, A., Krol, M., Frankenberg, C., Scheepmaker, R. A., Dlugokencky, E., Wofsy, S. C., Kort, E. A., Sweeney, C., Schuck, T., Brenninkmeijer, C., Chen, H., Beck, V. and Gerbig, C.: Atmospheric CH_4 in the first decade of the 21st century: Inverse modeling analysis using SCIAMACHY satellite retrievals and NOAA surface measurements, J. Geophys. Res. Atmos., 118(13), 7350–7369, doi:10.1002/jgrd.50480, 2013.

Bloom, A. A., Bowman, K. W., Lee, M., Turner, A. J., Schroeder, R., Worden, J. R., Weidner, R., McDonald, K. C. and Jacob, D. J.: A global wetland methane emissions and uncertainty dataset for atmospheric chemical transport models (WetCHARTs version 1.0), Geosci. Model Dev., 10(6), 2141–2156, doi:10.5194/gmd-10-2141-2017, 2017a.

Bloom, A. A., Bowman, K. W., Lee, M., Turner, A. J., Schroeder, R., Worden, J. R., Weidner, R. J., McDonald, K. C. and Jacob, D. J.: CMS: Global 0.5-deg Wetland Methane Emissions and Uncertainty (WetCHARTs v1.0), , doi:10.3334/ornldaac/1502, 2017b.

Bodesheim, P., Jung, M., Gans, F., Mahecha, M. D. and Reichstein, M.: Upscaled diurnal cycles of land–atmosphere fluxes: a new global half-hourly data product, Earth Syst. Sci. Data, 10(3), 1327–1365, doi:10.5194/essd-10-1327-2018, 2018.

Bohn, T. J., Melton, J. R., Ito, A., Kleinen, T., Spahni, R., Stocker, B. D., Zhang, B., Zhu, X., Schroeder, R., Glagolev, M. V, Maksyutov, S., Brovkin, V., Chen, G., Denisov, S. N., Eliseev, A. V, Gallego-Sala, A., McDonald, K. C., Rawlins, M. A., Riley, W. J., Subin, Z. M., Tian, H., Zhuang, Q. and Kaplan, J. O.: WETCHIMP-WSL: intercomparison of wetland methane emissions models over West Siberia, Biogeosciences, 12(11), 3321–3349, doi:10.5194/bg-12-3321-2015, 2015.

Breiman, L.: Random Forests, Mach. Learn., 45(1), 5–32, doi:10.1023/A:1010933404324, 2001.

Brown, J., Ferrians, O., Heginbottom, J. A. and Melnikov, E.: Circum-Arctic Map of Permafrost and Ground-Ice Conditions, Version 2. 45°N, 180°W; 90°N, 180°W. Boulder, Colorado USA. NSIDC: National Snow and Ice Data Center. Accessed December 29, 2016., 2002.

Brown, M. G., Humphreys, E. R., Moore, T. R., Roulet, N. T. and Lafleur, P. M.: Evidence for a nonmonotonic relationship between ecosystem-scale peatland methane emissions and water table depth, J. Geophys. Res. Biogeosciences, 119(5), 826–835, doi:10.1002/2013JG002576, 2014.

Bruhwiler, L., Dlugokencky, E., Masarie, K., Ishizawa, M., Andrews, A., Miller, J., Sweeney, C., Tans, P. and Worthy, D.: CarbonTracker-CH_4: an assimilation system for estimating emissions of atmospheric methane, Atmos. Chem. Phys., 14(16), 8269–8293, doi:10.5194/acp-14-8269-2014, 2014.

Chanton, J. P., Bauer, J. E., Glaser, P. A., Siegel, D. I., Kelley, C. A., Tyler, S. C., Romanowicz, E. H. and Lazrus, A.: Radiocarbon evidence for the substrates supporting methane formation within northern Minnesota peatlands, Geochim. Cosmochim. Acta, 59(17), 3663–3668, doi:http://dx.doi.org/10.1016/0016-7037(95)00240-Z, 1995.

Chen, X., Bohn, T. J. and Lettenmaier, D. P.: Model estimates of climate controls on pan-Arctic wetland methane emissions, Biogeosciences, 12(21), 6259–6277, doi:10.5194/bg-12-6259-2015, 2015.

Christensen, T. R., Ekberg, A., Ström, L., Mastepanov, M., Panikov, N., Öquist, M., Svensson, B. H., Nykänen, H., Martikainen, P. J. and Oskarsson, H.: Factors controlling large scale variations in methane emissions from wetlands, Geophys. Res. Lett., 30(7), n/a-n/a, doi:10.1029/2002GL016848, 2003.

Ciais, P., Sabine, C., Bala, G., Bopp, L., Brovkin, V., Canadell, J., Chhabra, A., DeFries, R., Galloway, J., Heimann, M., Jones, C., Le Quéré, C., Myneni, R. B., Piao, S. and Thornton, P.: Carbon and Other Biogeochemical Cycles, in Climate Change 2013: The Physical Science Basis. Contribution of Working Group I to the Fifth Assessment Report of the Intergovernmental Panel on Climate Change, edited by T. F. Stocker, D. Qin, G.-K. Plattner, M. Tignor, S. K. Allen, J. Boschung, A. Nauels, Y.

Xia, V. Bex, and P. M. Midgley, pp. 465–570, Cambridge University Press, Cambridge, United Kingdom and New York, NY, USA., 2013.

Davidson, J. S., Santos, J. M., Sloan, L. V., Reuss-Schmidt, K., Phoenix, K. G., Oechel, C. W. and Zona, D.: Upscaling CH_4 Fluxes Using High-Resolution Imagery in Arctic Tundra Ecosystems, Remote Sens. , 9(12), doi:10.3390/rs9121227, 2017.

Detto, M., Verfaillie, J., Anderson, F., Xu, L. and Baldocchi, D.: Comparing laser-based open- and closed-path gas analyzers to measure methane fluxes using the eddy covariance method, Agric. For. Meteorol., 151(10), 1312–1324, doi:http://dx.doi.org/10.1016/j.agrformet.2011.05.014, 2011.

Didan, K.: MOD13A3 MODIS/Terra vegetation Indices Monthly L3 Global 1km SIN Grid V006. NASA EOSDIS LP DAAC. doi: 10.5067/MODIS/MOD13A3.006, 2015.

Etminan, M., Myhre, G., Highwood, E. J. and Shine, K. P.: Radiative forcing of carbon dioxide, methane, and nitrous oxide: A significant revision of the methane radiative forcing, Geophys. Res. Lett., 43(24), 12,612-614,623, doi:10.1002/2016GL071930, 2016.

Euskirchen, E. S., Edgar, C. W., Turetsky, M. R., Waldrop, M. P. and Harden, J. W.: Differential response of carbon fluxes to climate in three peatland ecosystems that vary in the presence and stability of permafrost, J. Geophys. Res. Biogeosciences, 119(8), 1576–1595, doi:10.1002/2014JG002683, 2014.

Franz, D., Acosta, M., Altimir, N., Arriga, N., Arrouays, D., Aubinet, M., Aurela, M., Ayres, E., Lopez-Ballesteros, A., Barbaste, M., Berveiller, D., Biraud, S., Boukir, H., Brown, T., Bruemmer, C., Buchmann, N., Burba, G., Carrara, A., Cescatti, A., Ceschia, E., Clement, R., Cremonese, E., Crill, P., Darenova, E., Dengel, S., D'Odorico, P., Filippa, G., Fleck, S., Fratini, G., Fuss, R., Gielen, B., Gogo, S., Grace, J., Graf, A., Grelle, A., Gross, P., Gruenwald, T., Haapanala, S., Hehn, M., Heinesch, B., Heiskanen, J., Herbst, M., Herschlein, C., Hortnagl, L., Hufkens, K., Ibrom, A., Jolivet, C., Joly, L., Jones, M., Kiese, R., Klemedtsson, L., Kljun, N., Klumpp, K., Kolari, P., Kolle, O., Kowalski, A., Kutsch, W., Laurila, T., de Ligne, A., Linder, S., Lindroth, A., Lohila, A., Longdoz, B., Mammarella, I., Manise, T., Maranon Jimenez, S., Matteucci, G., Mauder, M., Meier, P., Merbold, L., Mereu, S., Metzger, S., Migliavacca, M., Molder, M., Montagnani, L., Moureaux, C., Nelson, D., Nemitz, E., Nicolini, G., Nilsson, M. B., de Beeck, M., Osborne, B., Lofvenius, M. O., Pavelka, M., Peichl, M., Peltola, O., Pihlatie, M., Pitacco, A., Pokorny, R., Pumpanen, J., Ratie, C., Rebmann, C., Roland, M., Sabbatini, S., Saby, N. P. A., Saunders, M., Schmid, H. P., Schrumpf, M., Sedlak, P., et al.: Towards long-term standardised carbon and greenhouse gas observations for monitoring Europe's terrestrial ecosystems: a review, Int. AGROPHYSICS, 32(4), 439+, doi:10.1515/intag-2017-0039, 2018.

Friborg, T., Christensen, T. R. and Søgaard, H.: Rapid response of greenhouse gas emission to early spring thaw in a subarctic mire as shown by micrometeorological techniques, Geophys. Res. Lett., 24(23), 3061–3064, doi:10.1029/97GL03024, 1997.

Glagolev, M., Kleptsova, I., Filippov, I., Maksyutov, S. and Machida, T.: Regional methane emission from West Siberia mire landscapes, Environ. Res. Lett., 6(4), 45214 [online] Available from: http://stacks.iop.org/1748-9326/6/i=4/a=045214, 2011.

Goodrich, J. P., Oechel, W. C., Gioli, B., Moreaux, V., Murphy, P. C., Burba, G. and Zona, D.: Impact of different eddy covariance sensors, site set-up, and maintenance on the annual balance of CO_2 and CH_4 in the harsh Arctic environment, Agric. For. Meteorol., 228–229, 239–251, doi:https://doi.org/10.1016/j.agrformet.2016.07.008, 2016.

Granberg, G., Mikkelä, C., Sundh, I., Svensson, B. H. and Nilsson, M.: Sources of spatial variation in methane emission from mires in northern Sweden: A mechanistic approach in statistical modeling, Global Biogeochem. Cycles, 11(2), 135–150, doi:10.1029/96GB03352, 1997.

Gray, A., Levy, P. E., Cooper, M. D. A., Jones, T., Gaiawyn, J., Leeson, S. R., Ward, S. E., Dinsmore, K. J., Drewer, J., Sheppard, L. J., Ostle, N. J., Evans, C. D., Burden, A. and Zieliński, P.: Methane indicator values for peatlands: a comparison of species and functional groups, Glob. Chang. Biol., 19(4), 1141–1150, doi:10.1111/gcb.12120, 2013.

Hall, D. K. and Riggs, G. A.: MODIS/Terra Snow Cover Monthly L3 Global 0.05Deg CMG, Version 6. 45°N, 180°W; 90°N, 180°E. Boulder, Colorado USA. NASA National Snow and Ice Data Center Distributed Active Archive Center. doi: https://doi.org/10.5067/MODIS/MOD10CM.006. Accessed August 24, 2015.

Hall, D. K. and Riggs, G. A.: MODIS/Terra Snow Cover Daily L3 Global 500m Grid, Version 6. Boulder, Colorado USA. NASA National Snow and Ice Data Center Distributed Active Archive Center. doi: https://doi.org/10.5067/MODIS/MOD10A1.006. Accessed November 29, 2018., 2016.

Hanis, K. L., Tenuta, M., Amiro, B. D. and Papakyriakou, T. N.: Seasonal dynamics of methane emissions from a subarctic fen in the Hudson Bay Lowlands, Biogeosciences, 10(7), 4465–4479, doi:10.5194/bg-10-4465-2013, 2013.

Hargrove, W. W., Hoffman, F. M. and Law, B. E.: New analysis reveals representativeness of the AmeriFlux network, Eos, Trans. Am. Geophys. Union, 84(48), 529–535, doi:10.1029/2003EO480001, 2003.

Helbig, M., Chasmer, L. E., Kljun, N., Quinton, W. L., Treat, C. C. and Sonnentag, O.: The positive net radiative greenhouse gas forcing of increasing methane emissions from a thawing boreal forest-wetland landscape, Glob. Chang. Biol., 23(6), 2413–2427, doi:10.1111/gcb.13520, 2016.

Helbig, M., Quinton, W. L. and Sonnentag, O.: Warmer spring conditions increase annual methane emissions from a boreal peat landscape with sporadic permafrost, Environ. Res. Lett., 12(11), doi:10.1088/1748-9326/aa8c85, 2017.

Hoffman, F. M., Kumar, J., Mills, R. T. and Hargrove, W. W.: Representativeness-based sampling network design for the State of Alaska, Landsc. Ecol., 28(8), 1567–1586, doi:10.1007/s10980-013-9902-0, 2013.

Hommeltenberg, J., Mauder, M., Drösler, M., Heidbach, K., Werle, P. and Schmid, H. P.: Ecosystem scale methane fluxes in a natural temperate bog-pine forest in southern Germany, Agric. For. Meteorol., 198–199, 273–284, doi:https://doi.org/10.1016/j.agrformet.2014.08.017, 2014.

Jackowicz-Korczyński, M., Christensen, T. R., Bäckstrand, K., Crill, P., Friborg, T., Mastepanov, M. and Ström, L.: Annual cycle of methane emission from a subarctic peatland, J. Geophys. Res. Biogeosciences, 115(G2), G02009, doi:10.1029/2008JG000913, 2010.

Jammet, M., Dengel, S., Kettner, E., Parmentier, F.-J. W., Wik, M., Crill, P. and Friborg, T.: Year-round CH_4 and CO_2 flux dynamics in two contrasting freshwater ecosystems of the subarctic, Biogeosciences, 14(22), 5189–5216, doi:10.5194/bg-14-5189-2017, 2017.

Jet Propulsion Laboratory: ISLSCP II Land and Water Masks with Ancillary Data. Data set. Available on-line [http://daac.ornl.gov/] from Oak Ridge National Laboratory Distributed Active Archive Center, Oak Ridge, Tennessee, USA. http://dx.doi.org/10.3334/ORNLDAAC/1200, 2013.

Joabsson, A. and Christensen, T. R.: Methane emissions from wetlands and their relationship with vascular plants: an Arctic example, Glob. Chang. Biol., 7(8), 919–932, doi:10.1046/j.1354-1013.2001.00044.x, 2002.

Jung, M., Reichstein, M., Ciais, P., Seneviratne, S. I., Sheffield, J., Goulden, M. L., Bonan, G., Cescatti, A., Chen, J., de Jeu, R., Dolman, A. J., Eugster, W., Gerten, D., Gianelle, D., Gobron, N., Heinke, J., Kimball, J., Law, B. E., Montagnani, L., Mu, Q., Mueller, B., Oleson, K., Papale, D., Richardson, A. D., Roupsard, O., Running, S., Tomelleri, E., Viovy, N., Weber, U., Williams, C., Wood, E., Zaehle, S. and Zhang, K.: Recent decline in the global land evapotranspiration trend due to limited moisture supply, Nature, 467(7318), 951–954, doi:http://www.nature.com/nature/journal/v467/n7318/abs/nature09396.html#supplementary-information, 2010.

Jung, M., Reichstein, M., Margolis, H. A., Cescatti, A., Richardson, A. D., Arain, M. A., Arneth, A., Bernhofer, C., Bonal, D., Chen, J., Gianelle, D., Gobron, N., Kiely, G., Kutsch, W., Lasslop, G., Law, B. E., Lindroth, A., Merbold, L., Montagnani, L., Moors, E. J., Papale, D., Sottocornola, M., Vaccari, F. and Williams, C.: Global patterns of land-atmosphere fluxes of carbon dioxide, latent heat, and sensible heat derived from eddy covariance, satellite, and meteorological observations, J. Geophys. Res. Biogeosciences, 116(G3), doi:10.1029/2010JG001566, 2011.

Jung, M., Reichstein, M., Schwalm, C. R., Huntingford, C., Sitch, S., Ahlström, A., Arneth, A., Camps-Valls, G., Ciais, P., Friedlingstein, P., Gans, F., Ichii, K., Jain, A. K., Kato, E., Papale, D., Poulter, B., Raduly, B., Rödenbeck, C., Tramontana, G., Viovy, N., Wang, Y.-P., Weber, U., Zaehle, S. and Zeng, N.: Compensatory water effects link yearly global land CO_2 sink changes to temperature, Nature, 541, 516 [online] Available from: http://dx.doi.org/10.1038/nature20780, 2017.

Kim, H.-S., Maksyutov, S., Glagolev, M. V, Machida, T., Patra, P. K., Sudo, K. and Inoue, G.: Evaluation of methane emissions from West Siberian wetlands based on inverse modeling, Environ. Res. Lett., 6(3), 35201 [online] Available from: http://stacks.iop.org/1748-9326/6/i=3/a=035201, 2011.

Kim, J., Verma, S. B. and Billesbach, D. P.: Seasonal variation in methane emission from a temperate Phragmites-dominated marsh: effect of growth stage and plant-mediated transport, Glob. Chang. Biol., 5(4), 433–440, doi:10.1046/j.1365-2486.1999.00237.x, 1999.

Kittler, F., Eugster, W., Foken, T., Heimann, M., Kolle, O. and Göckede, M.: High-quality eddy-covariance CO_2 budgets under cold climate conditions, J. Geophys. Res. Biogeosciences, 122(8), 2064–2084, doi:10.1002/2017JG003830, 2017a.

Kittler, F., Heimann, M., Kolle, O., Zimov, N., Zimov, S. and Göckede, M.: Long-Term Drainage Reduces CO_2 Uptake and CH_4 Emissions in a Siberian Permafrost Ecosystem, Global Biogeochem. Cycles, 31(12), 1704–1717, doi:10.1002/2017GB005774, 2017b.

Knoblauch, C., Spott, O., Evgrafova, S., Kutzbach, L. and Pfeiffer, E.-M.: Regulation of methane production, oxidation, and emission by vascular plants and bryophytes in ponds of the northeast Siberian polygonal tundra, J. Geophys. Res. Biogeosciences, n/a-n/a, doi:10.1002/2015JG003053, 2015.

Knox, S. H., Jackson, R. B., Poulter, B., McNicol, G., Fluet-Chouinard, E., Zhang, Z., Hugelius, G., Bousquet, P., Canadell, J. G., Saunois, M., Papale, D., Chu, H., Keenan, T. F., Baldocchi, D. D., Mammarella, I., Aurela, M., Bohrer, G., Campbell, D., Cescatti, A., Chamberlain, S., Chen, J., Dengel, S., Desai, A. R., Euskirchen, E. S., Friborg, T., Göckede, M., Heimann, M., Helbig, M., Kang, M., Klatt, J., Krauss, K. W., Kutzbach, L., Lohila, A., Mitra, B., Morin, T. H., Nilsson, M. B., Niu, S., Noormets, A., Oechel, W. C., Peichl, M., Peltola, O., Reba, M. L., Runkle, B. R. K., Ryu, Y., Sachs, T., Schäfer, K. V. R., Shurpali, N., Sonnentag, O., Tang, A. C. I., Vesala, T., Ward, E. J., Windham-Myers, L. and Zona, D.: FLUXNET-CH_4 Synthesis Activity: Objectives, Observations, and Future Directions, Bull. Am. Meteorol. Soc., in review.

Korrensalo, A., Männistö, E., Alekseychik, P., Mammarella, I., Rinne, J., Vesala, T. and Tuittila, E.-S.: Small spatial variability in methane emission measured from a wet patterned boreal bog, Biogeosciences, 15(6), 1749–1761, doi:10.5194/bg-15-1749-2018, 2018.

Kowalska, N., Chojnicki, B. H., Rinne, J., Haapanala, S., Siedlecki, P., Urbaniak, M., Juszczak, R. and Olejnik, J.: Measurements of methane emission from a temperate wetland by the eddy covariance method, Int. Agrophysics, 27(3), 283–290, doi:https://doi.org/10.2478/v10247-012-0096-5, 2013.

Kwon, M. J., Beulig, F., Ilie, I., Wildner, M., Küsel, K., Merbold, L., Mahecha, M. D., Zimov, N., Zimov, S. A., Heimann, M., Schuur, E. A. G., Kostka, J. E., Kolle, O., Hilke, I. and Göckede, M.: Plants, microorganisms, and soil temperatures contribute to a decrease in methane fluxes on a drained Arctic floodplain, Glob. Chang. Biol., 23(6), 2396–2412, doi:10.1111/gcb.13558, 2017.

Larmola, T., Tuittila, E.-S., Tiirola, M., Nykänen, H., Martikainen, P. J., Yrjälä, K., Tuomivirta, T. and Fritze, H.: The role of Sphagnum mosses in the methane cycling of a boreal mire, Ecology, 91(8), 2356–2365, doi:10.1890/09-1343.1, 2010.

Lasslop, G., Reichstein, M., Papale, D., Richardson, A. D., Arneth, A., Barr, A., Stoy, P. and Wohlfahrt, G.: Separation of net ecosystem exchange into assimilation and respiration using a light response curve approach: critical issues and global evaluation, Glob. Chang. Biol., 16(1), 187–208, doi:10.1111/j.1365-2486.2009.02041.x, 2009.

Lees, K. J., Quaife, T., Artz, R. R. E., Khomik, M. and Clark, J. M.: Potential for using remote sensing to estimate carbon fluxes across northern peatlands – A review, Sci. Total Environ., 615, 857–874, doi:https://doi.org/10.1016/j.scitotenv.2017.09.103, 2018.

Lehner, B. and Döll, P.: Development and validation of a global database of lakes, reservoirs and wetlands, J. Hydrol., 296(1), 1–22, doi:https://doi.org/10.1016/j.jhydrol.2004.03.028, 2004.

Li, T., Raivonen, M., Alekseychik, P., Aurela, M., Lohila, A., Zheng, X., Zhang, Q., Wang, G., Mammarella, I., Rinne, J., Yu, L., Xie, B., Vesala, T. and Zhang, W.: Importance of vegetation classes in modeling CH_4 emissions from boreal and subarctic wetlands in Finland, Sci. Total Environ., 572, 1111–1122, doi:https://doi.org/10.1016/j.scitotenv.2016.08.020, 2016.

Liebner, S., Zeyer, J., Wagner, D., Schubert, C., Pfeiffer, E.-M. and Knoblauch, C.: Methane oxidation associated with submerged brown mosses reduces methane emissions from Siberian polygonal tundra, J. Ecol., 99(4), 914–922, doi:10.1111/j.1365-2745.2011.01823.x, 2011.

Long, K. D., Flanagan, L. B. and Cai, T.: Diurnal and seasonal variation in methane emissions in a northern Canadian peatland measured by eddy covariance, Glob. Chang. Biol., 16(9), 2420–2435, doi:10.1111/j.1365-2486.2009.02083.x, 2010.

Mahecha, M. D., Reichstein, M., Carvalhais, N., Lasslop, G., Lange, H., Seneviratne, S. I., Vargas, R., Ammann, C., Arain, M. A., Cescatti, A., Janssens, I. A., Migliavacca, M., Montagnani, L. and Richardson, A. D.: Global Convergence in the Temperature Sensitivity of Respiration at Ecosystem Level, Science (80-.)., 329(5993), 838 [online] Available from: http://science.sciencemag.org/content/329/5993/838.abstract, 2010.

Mammarella, I., Peltola, O., Nordbo, A., Järvi, L. and Rannik, Ü.: Quantifying the uncertainty of eddy covariance fluxes due to the use of different software packages and combinations of processing steps in two contrasting ecosystems, Atmos. Meas. Tech., 9(10), 4915–4933, doi:10.5194/amt-9-4915-2016, 2016.

Marushchak, M. E., Friborg, T., Biasi, C., Herbst, M., Johansson, T., Kiepe, I., Liimatainen, M., Lind, S. E., Martikainen, P. J., Virtanen, T., Soegaard, H. and Shurpali, N. J.: Methane dynamics in the subarctic tundra: combining stable isotope analyses, plot- and ecosystem-scale flux measurements, Biogeosciences, 13(2), 597–608, doi:10.5194/bg-13-597-2016, 2016.

Mastepanov, M., Sigsgaard, C., Dlugokencky, E. J., Houweling, S., Ström, L., Tamstorf, M. P. and Christensen, T. R.: Large tundra methane burst during onset of freezing, Nature, 456, 628 [online] Available from: http://dx.doi.org/10.1038/nature07464, 2008.

Mastepanov, M., Sigsgaard, C., Tagesson, T., Ström, L., Tamstorf, M. P., Lund, M. and Christensen, T. R.: Revisiting factors controlling methane emissions from high-Arctic tundra, Biogeosciences, 10(7), 5139–5158, doi:10.5194/bg-10-5139-2013, 2013.

Mauder, M., Cuntz, M., Druee, C., Graf, A., Rebmann, C., Schmid, H. P., Schmidt, M. and Steinbrecher, R.: A strategy for quality and uncertainty assessment of long-term eddy-covariance measurements, Agric. For. Meteorol., 169, 122–135, doi:10.1016/j.agrformet.2012.09.006, 2013.

McDermitt, D., Burba, G., Xu, L., Anderson, T., Komissarov, A., Riensche, B., Schedlbauer, J., Starr, G., Zona, D., Oechel, W., Oberbauer, S. and Hastings, S.: A new low-power, open-path instrument for measuring methane flux by eddy covariance, Appl. Phys. B Lasers Opt., doi:10.1007/s00340-010-4307-0, 2010.

McEwing, K., Fisher, J. and Zona, D.: Environmental and vegetation controls on the spatial variability of CH_4 emission from wet-sedge and tussock tundra ecosystems in the Arctic, Plant Soil, 388(1–2), 37–52, doi:10.1007/s11104-014-2377-1, 2015.

McNorton, J., Gloor, E., Wilson, C., Hayman, G. D., Gedney, N., Comyn-Platt, E., Marthews, T., Parker, R. J., Boesch, H. and Chipperfield, M. P.: Role of regional wetland emissions in atmospheric methane variability, Geophys. Res. Lett., 43(21), 11,411-433,444, doi:doi:10.1002/2016GL070649, 2016.

Meingast, K. M., Falkowski, M. J., Kane, E. S., Potvin, L. R., Benscoter, B. W., Smith, A. M. S., Bourgeau-Chavez, L. L. and Miller, M. E.: Spectral detection of near-surface moisture content and water-table position in northern peatland ecosystems, Remote Sens. Environ., 152, 536–546, doi:https://doi.org/10.1016/j.rse.2014.07.014, 2014.

Melton, J. R., Wania, R., Hodson, E. L., Poulter, B., Ringeval, B., Spahni, R., Bohn, T., Avis, C. A., Beerling, D. J., Chen, G., Eliseev, A. V, Denisov, S. N., Hopcroft, P. O., Lettenmaier, D. P., Riley, W. J., Singarayer, J. S., Subin, Z. M., Tian, H.,

Zürcher, S., Brovkin, V., van Bodegom, P. M., Kleinen, T., Yu, Z. C. and Kaplan, J. O.: Present state of global wetland extent and wetland methane modelling: conclusions from a model inter-comparison project (WETCHIMP), Biogeosciences, 10(2), 753–788, doi:10.5194/bg-10-753-2013, 2013.

Le Mer, J. and Roger, P.: Production, oxidation, emission and consumption of methane by soils: A review, Eur. J. Soil Biol., 37(1), 25–50, doi:http://dx.doi.org/10.1016/S1164-5563(01)01067-6, 2001.

Miller, S. M., Worthy, D. E. J., Michalak, A. M., Wofsy, S. C., Kort, E. A., Havice, T. C., Andrews, A. E., Dlugokencky, E. J., Kaplan, J. O., Levi, P. J., Tian, H. and Zhang, B.: Observational constraints on the distribution, seasonality, and environmental predictors of North American boreal methane emissions, Global Biogeochem. Cycles, 28(2), 146–160, doi:10.1002/2013GB004580, 2014.

Moffat, A. M., Beckstein, C., Churkina, G., Mund, M. and Heimann, M.: Characterization of ecosystem responses to climatic controls using artificial neural networks, Glob. Chang. Biol., 16(10), 2737–2749, doi:10.1111/j.1365-2486.2010.02171.x, 2010.

Nadeau, D. F., Rousseau, A. N., Coursolle, C., Margolis, H. A. and Parlange, M. B.: Summer methane fluxes from a boreal bog in northern Quebec, Canada, using eddy covariance measurements, Atmos. Environ., 81, 464–474, doi:http://dx.doi.org/10.1016/j.atmosenv.2013.09.044, 2013.

Nash, J. E. and Sutcliffe, J. V: River flow forecasting through conceptual models part I — A discussion of principles, J. Hydrol., 10(3), 282–290, doi:https://doi.org/10.1016/0022-1694(70)90255-6, 1970.

Nemitz, E., Mammarella, I., Ibrom, A., Aurela, M., Burba, G. G., Dengel, S., Gielen, B., Grelle, A., Heinesch, B., Herbst, M., Hörtnagl, L., Klemedtsson, L., Lindroth, A., Lohila, A., McDermitt, D. K., Meier, P., Merbold, L., Nelson, D., Nicolini, G., Nilsson, M. B., Peltola, O., Rinne, J. and Zahniser, M.: Standardisation of eddy-covariance flux measurements of methane and nitrous oxide, Int. Agrophysics, 32(4), 517–549 [online] Available from: http://nora.nerc.ac.uk/id/eprint/521848/, 2018.

Nilsson, M. B., Sagerfors, J., Buffam, I., Laudon, H., Eriksson, T., Grelle, A., Klemedtsson, L., Weslien, P. and Lindroth, A.: Contemporary carbon accumulation in a boreal oligotrophic minerogenic mire – a significant sink after accounting for all C-fluxes, Glob. Chang. Biol., 14(10), 2317–2332, doi:10.1111/j.1365-2486.2008.01654.x, 2008.

Olefeldt, D., Turetsky, M. R., Crill, P. M. and McGuire, A. D.: Environmental and physical controls on northern terrestrial methane emissions across permafrost zones, Glob. Chang. Biol., 19(2), 589–603, doi:10.1111/gcb.12071, 2012.

Olson, D. M., Dinerstein, E., Wikramanayake, E. D., Burgess, N. D., Powell, G. V. N., Underwood, E. C., D'amico, J. A., Itoua, I., Strand, H. E., Morrison, J. C., Loucks, C. J., Allnutt, T. F., Ricketts, T. H., Kura, Y., Lamoreux, J. F., Wettengel, W. W., Hedao, P. and Kassem, K. R.: Terrestrial Ecoregions of the World: A New Map of Life on EarthA new global map of terrestrial ecoregions provides an innovative tool for conserving biodiversity, Bioscience, 51(11), 933–938 [online] Available from: http://dx.doi.org/10.1641/0006-3568(2001)051[0933:TEOTWA]2.0.CO, 2001.

Papale, D., Black, T. A., Carvalhais, N., Cescatti, A., Chen, J., Jung, M., Kiely, G., Lasslop, G., Mahecha, M. D., Margolis, H., Merbold, L., Montagnani, L., Moors, E., Olesen, J. E., Reichstein, M., Tramontana, G., Gorsel, E., Wohlfahrt, G. and

Ráduly, B.: Effect of spatial sampling from European flux towers for estimating carbon and water fluxes with artificial neural networks, J. Geophys. Res. Biogeosciences, 120(10), 1941–1957, doi:10.1002/2015JG002997, 2015.

Parmentier, F. J. W., van Huissteden, J., van der Molen, M. K., Schaepman-Strub, G., Karsanaev, S. A., Maximov, T. C. and Dolman, A. J.: Spatial and temporal dynamics in eddy covariance observations of methane fluxes at a tundra site in northeastern Siberia, J. Geophys. Res. Biogeosciences, 116(G3), doi:10.1029/2010JG001637, 2011a.

Parmentier, F. J. W., van Huissteden, J., Kip, N., Op den Camp, H. J. M., Jetten, M. S. M., Maximov, T. C. and Dolman, A. J.: The role of endophytic methane-oxidizing bacteria in submerged <I>Sphagnum</I> in determining methane emissions of Northeastern Siberian tundra, Biogeosciences, 8(5), 1267–1278, doi:10.5194/bg-8-1267-2011, 2011b.

Peltola, O., Mammarella, I., Haapanala, S., Burba, G. and Vesala, T.: Field intercomparison of four methane gas analyzers suitable for eddy covariance flux measurements, Biogeosciences, 10, 3749–3765, doi:10.5194/bg-10-3749-2013, 2013.

Peltola, O., Hensen, A., Helfter, C., Belelli Marchesini, L., Bosveld, F., van den Bulk, P., Elbers, J., Haapanala, S., Holst, J., Laurila, T., Lindroth, A., Nemitz, E., Röckmann, T., Vermeulen, A. and Mammarella, I.: Evaluating the performance of commonly used gas analysers for methane eddy covariance flux measurements: the InGOS inter-comparison field experiment, Biogeosciences, 11, 3163–3186, doi:10.5194/bg-11-3163-2014, 2014.

Peltola, O., Vesala, T., Gao, Y., Räty, O., Alekseychik, P., Aurela, M., Chojnicki, B., Desai, A., Dolman, H., Euskirchen, E., Friborg, T., Göckede, M., Helbig, M., Humphreys, E., Jackson, R., Jocher, G., Joos, F., Klatt, J., Knox, S., Kowalska, N., Kutzbach, L., Lienert, S., Lohila, A., Mammarella, I., Nadeau, D., Nilsson, M., Oechel, W., Peichl, M., Pypker, T., Quinton, W., Rinne, J., Sachs, T., Samson, M., Schmid, H. P., Sonnentag, O., Wille, C., Zona, D. and Aalto, T.: Dataset for "Monthly Gridded Data Product of Northern Wetland Methane Emissions Based on Upscaling Eddy Covariance Observations," , doi: 10.5281/zenodo.2560163, 2019.

Petrescu, A. M. R., van Beek, L. P. H., van Huissteden, J., Prigent, C., Sachs, T., Corradi, C. A. R., Parmentier, F. J. W. and Dolman, A. J.: Modeling regional to global CH_4 emissions of boreal and arctic wetlands, Global Biogeochem. Cycles, 24(4), doi:10.1029/2009GB003610, 2010.

Petrescu, A. M. R., Lohila, A., Tuovinen, J.-P., Baldocchi, D. D., Desai, A. R., Roulet, N. T., Vesala, T., Dolman, A. J., Oechel, W. C., Marcolla, B., Friborg, T., Rinne, J., Matthes, J. H., Merbold, L., Meijide, A., Kiely, G., Sottocornola, M., Sachs, T., Zona, D., Varlagin, A., Lai, D. Y. F., Veenendaal, E., Parmentier, F.-J. W., Skiba, U., Lund, M., Hensen, A., van Huissteden, J., Flanagan, L. B., Shurpali, N. J., Grünwald, T., Humphreys, E. R., Jackowicz-Korczyński, M., Aurela, M. A., Laurila, T., Grüning, C., Corradi, C. A. R., Schrier-Uijl, A. P., Christensen, T. R., Tamstorf, M. P., Mastepanov, M., Martikainen, P. J., Verma, S. B., Bernhofer, C. and Cescatti, A.: The uncertain climate footprint of wetlands under human pressure, Proc. Natl. Acad. Sci., 112(15), 4594–4599, doi:10.1073/pnas.1416267112, 2015.

Pickett-Heaps, C. A., Jacob, D. J., Wecht, K. J., Kort, E. A., Wofsy, S. C., Diskin, G. S., Worthy, D. E. J., Kaplan, J. O., Bey, I. and Drevet, J.: Magnitude and seasonality of wetland methane emissions from the Hudson Bay Lowlands (Canada), Atmos. Chem. Phys., 11(8), 3773–3779, doi:10.5194/acp-11-3773-2011, 2011.

Proctor, C. and He, Y.: Quantifying root extracts and exudates of sedge and shrub in relation to root morphology, Soil Biol. Biochem., 114, 168–180, doi:https://doi.org/10.1016/j.soilbio.2017.07.006, 2017.

Pugh, C. A., Reed, D. E., Desai, A. R. and Sulman, B. N.: Wetland flux controls: how does interacting water table levels and temperature influence carbon dioxide and methane fluxes in northern Wisconsin?, Biogeochemistry, 137(1–2), 15–25, doi:10.1007/s10533-017-0414-x, 2018.

Pypker, T. G., Moore, P. A., Waddington, J. M., Hribljan, J. A. and Chimner, R. C.: Shifting environmental controls on CH_4 fluxes in a sub-boreal peatland, Biogeosciences, 10(12), 7971–7981, doi:10.5194/bg-10-7971-2013, 2013.

Raghoebarsing, A. A., Smolders, A. J. P., Schmid, M. C., Rijpstra, W. I. C., Wolters-Arts, M., Derksen, J., Jetten, M. S. M., Schouten, S., Sinninghe Damsté, J. S., Lamers, L. P. M., Roelofs, J. G. M., Op den Camp, H. J. M. and Strous, M.: Methanotrophic symbionts provide carbon for photosynthesis in peat bogs, Nature, 436, 1153 [online] Available from: http://dx.doi.org/10.1038/nature03802, 2005.

Räisänen, J. and Räty, O.: Projections of daily mean temperature variability in the future: cross-validation tests with ENSEMBLES regional climate simulations, Clim. Dyn., 41(5), 1553–1568, doi:10.1007/s00382-012-1515-9, 2013.

Räty, O., Räisänen, J. and Ylhäisi, J. S.: Evaluation of delta change and bias correction methods for future daily precipitation: intermodel cross-validation using ENSEMBLES simulations, Clim. Dyn., 42(9), 2287–2303, doi:10.1007/s00382-014-2130-8, 2014.

Reichstein, M., Falge, E., Baldocchi, D., Papale, D., Aubinet, M., Berbigier, P., Bernhofer, C., Buchmann, N., Gilmanov, T., Granier, A., Grünwald, T., Havránková, K., Ilvesniemi, H., Janous, D., Knohl, A., Laurila, T., Lohila, A., Loustau, D., Matteucci, G., Meyers, T., Miglietta, F., Ourcival, J.-M., Pumpanen, J., Rambal, S., Rotenberg, E., Sanz, M., Tenhunen, J., Seufert, G., Vaccari, F., Vesala, T., Yakir, D. and Valentini, R.: On the separation of net ecosystem exchange into assimilation and ecosystem respiration: review and improved algorithm, Glob. Chang. Biol., 11(9), 1424–1439, doi:10.1111/j.1365-2486.2005.001002.x, 2005.

Rinne, J., Tuittila, E.-S., Peltola, O., Li, X., Raivonen, M., Alekseychik, P., Haapanala, S., Pihlatie, M., Aurela, M., Mammarella, I. and Vesala, T.: Temporal Variation of Ecosystem Scale Methane Emission From a Boreal Fen in Relation to Temperature, Water Table Position, and Carbon Dioxide Fluxes, Global Biogeochem. Cycles, 32(7), 1087–1106, doi:10.1029/2017GB005747, 2018.

Roberts, D. R., Bahn, V., Ciuti, S., Boyce, M. S., Elith, J., Guillera-Arroita, G., Hauenstein, S., Lahoz-Monfort, J. J., Schröder, B., Thuiller, W., Warton, D. I., Wintle, B. A., Hartig, F. and Dormann, C. F.: Cross-validation strategies for data with temporal, spatial, hierarchical, or phylogenetic structure, Ecography (Cop.)., 40(8), 913–929, doi:10.1111/ecog.02881, 2016.

Sachs, T., Wille, C., Boike, J. and Kutzbach, L.: Environmental controls on ecosystem-scale CH_4 emission from polygonal tundra in the Lena River Delta, Siberia, J. Geophys. Res. Biogeosciences, 113(G3), n/a-n/a, doi:10.1029/2007JG000505, 2008.

Sachs, T., Giebels, M., Boike, J. and Kutzbach, L.: Environmental controls on CH_4 emission from polygonal tundra on the microsite scale in the Lena river delta, Siberia, Glob. Chang. Biol., 16(11), 3096–3110, doi:10.1111/j.1365-2486.2010.02232.x, 2010.

Saunois, M., Bousquet, P., Poulter, B., Peregon, A., Ciais, P., Canadell, J. G., Dlugokencky, E. J., Etiope, G., Bastviken, D., Houweling, S., Janssens-Maenhout, G., Tubiello, F. N., Castaldi, S., Jackson, R. B., Alexe, M., Arora, V. K., Beerling, D. J., Bergamaschi, P., Blake, D. R., Brailsford, G., Brovkin, V., Bruhwiler, L., Crevoisier, C., Crill, P., Covey, K., Curry, C., Frankenberg, C., Gedney, N., Höglund-Isaksson, L., Ishizawa, M., Ito, A., Joos, F., Kim, H.-S., Kleinen, T., Krummel, P., Lamarque, J.-F., Langenfelds, R., Locatelli, R., Machida, T., Maksyutov, S., McDonald, K. C., Marshall, J., Melton, J. R., Morino, I., Naik, V., O'Doherty, S., Parmentier, F.-J. W., Patra, P. K., Peng, C., Peng, S., Peters, G. P., Pison, I., Prigent, C., Prinn, R., Ramonet, M., Riley, W. J., Saito, M., Santini, M., Schroeder, R., Simpson, I. J., Spahni, R., Steele, P., Takizawa, A., Thornton, B. F., Tian, H., Tohjima, Y., Viovy, N., Voulgarakis, A., van Weele, M., van der Werf, G. R., Weiss, R., Wiedinmyer, C., Wilton, D. J., Wiltshire, A., Worthy, D., Wunch, D., Xu, X., Yoshida, Y., Zhang, B., Zhang, Z. and Zhu, Q.: The global methane budget 2000–2012, Earth Syst. Sci. Data, 8(2), 697–751, doi:10.5194/essd-8-697-2016, 2016.

Saunois, M., Bousquet, P., Poulter, B., Peregon, A., Ciais, P., Canadell, J. G., Dlugokencky, E. J., Etiope, G., Bastviken, D., Houweling, S., Janssens-Maenhout, G., Tubiello, F. N., Castaldi, S., Jackson, R. B., Alexe, M., Arora, V. K., Beerling, D. J., Bergamaschi, P., Blake, D. R., Brailsford, G., Bruhwiler, L., Crevoisier, C., Crill, P., Covey, K., Frankenberg, C., Gedney, N., Höglund-Isaksson, L., Ishizawa, M., Ito, A., Joos, F., Kim, H.-S., Kleinen, T., Krummel, P., Lamarque, J.-F., Langenfelds, R., Locatelli, R., Machida, T., Maksyutov, S., Melton, J. R., Morino, I., Naik, V., O'Doherty, S., Parmentier, F.-J. W., Patra, P. K., Peng, C., Peng, S., Peters, G. P., Pison, I., Prinn, R., Ramonet, M., Riley, W. J., Saito, M., Santini, M., Schroeder, R., Simpson, I. J., Spahni, R., Takizawa, A., Thornton, B. F., Tian, H., Tohjima, Y., Viovy, N., Voulgarakis, A., Weiss, R., Wilton, D. J., Wiltshire, A., Worthy, D., Wunch, D., Xu, X., Yoshida, Y., Zhang, B., Zhang, Z. and Zhu, Q.: Variability and quasi-decadal changes in the methane budget over the period 2000–2012, Atmos. Chem. Phys., 17(18), 11135–11161, doi:10.5194/acp-17-11135-2017, 2017.

Schaller, C., Göckede, M. and Foken, T.: Flux calculation of short turbulent events – comparison of three methods, Atmos. Meas. Tech., 10(3), 869–880, doi:10.5194/amt-10-869-2017, 2017.

Schubert, P., Eklundh, L., Lund, M. and Nilsson, M.: Estimating northern peatland CO_2 exchange from MODIS time series data, Remote Sens. Environ., 114(6), 1178–1189, doi:https://doi.org/10.1016/j.rse.2010.01.005, 2010.

Schuur, E. A. G., McGuire, A. D., Schädel, C., Grosse, G., Harden, J. W., Hayes, D. J., Hugelius, G., Koven, C. D., Kuhry, P., Lawrence, D. M., Natali, S. M., Olefeldt, D., Romanovsky, V. E., Schaefer, K., Turetsky, M. R., Treat, C. C. and Vonk, J. E.: Climate change and the permafrost carbon feedback, Nature, 520, 171 [online] Available from: http://dx.doi.org/10.1038/nature14338, 2015.

Sims, D. A., Rahman, A. F., Cordova, V. D., El-Masri, B. Z., Baldocchi, D. D., Bolstad, P. V, Flanagan, L. B., Goldstein, A. H., Hollinger, D. Y., Misson, L., Monson, R. K., Oechel, W. C., Schmid, H. P., Wofsy, S. C. and Xu, L.: A new model of gross primary productivity for North American ecosystems based solely on the enhanced vegetation index and land surface temperature from MODIS, Remote Sens. Environ., 112(4), 1633–1646, doi:https://doi.org/10.1016/j.rse.2007.08.004, 2008.

Spahni, R., Wania, R., Neef, L., van Weele, M., Pison, I., Bousquet, P., Frankenberg, C., Foster, P. N., Joos, F., Prentice, I. C. and van Velthoven, P.: Constraining global methane emissions and uptake by ecosystems, Biogeosciences, 8(6), 1643–1665, doi:10.5194/bg-8-1643-2011, 2011.

Spahni, R., Joos, F., Stocker, B. D., Steinacher, M. and Yu, Z. C.: Transient simulations of the carbon and nitrogen dynamics in northern peatlands: from the Last Glacial Maximum to the 21st century, Clim. Past, 9(3), 1287–1308, doi:10.5194/cp-9-1287-2013, 2013.

Stocker, B. D., Roth, R., Joos, F., Spahni, R., Steinacher, M., Zaehle, S., Bouwman, L., Xu-Ri and Prentice, I. C.: Multiple greenhouse-gas feedbacks from the land biosphere under future climate change scenarios, Nat. Clim. Chang., 3, 666 [online] Available from: http://dx.doi.org/10.1038/nclimate1864, 2013.

Stocker, B. D., Spahni, R. and Joos, F.: DYPTOP: a cost-efficient TOPMODEL implementation to simulate sub-grid spatio-temporal dynamics of global wetlands and peatlands, Geosci. Model Dev., 7(6), 3089–3110, doi:10.5194/gmd-7-3089-2014, 2014.

Ström, L., Ekberg, A., Mastepanov, M. and Røjle Christensen, T.: The effect of vascular plants on carbon turnover and methane emissions from a tundra wetland, Glob. Chang. Biol., 9(8), 1185–1192, doi:10.1046/j.1365-2486.2003.00655.x, 2003.

Ström, L., Tagesson, T., Mastepanov, M. and Christensen, T. R.: Presence of Eriophorum scheuchzeri enhances substrate availability and methane emission in an Arctic wetland, Soil Biol. Biochem., 45, 61–70, doi:https://doi.org/10.1016/j.soilbio.2011.09.005, 2012.

Sulkava, M., Luyssaert, S., Zaehle, S. and Papale, D.: Assessing and improving the representativeness of monitoring networks: The European flux tower network example, J. Geophys. Res. Biogeosciences, 116(G3), doi:10.1029/2010JG001562, 2011.

Sun, Y., Frankenberg, C., Wood, J. D., Schimel, D. S., Jung, M., Guanter, L., Drewry, D. T., Verma, M., Porcar-Castell, A., Griffis, T. J., Gu, L., Magney, T. S., Köhler, P., Evans, B. and Yuen, K.: OCO-2 advances photosynthesis observation from space via solar-induced chlorophyll fluorescence, Science (80-.)., 358(6360) [online] Available from: http://science.sciencemag.org/content/358/6360/eaam5747.abstract, 2017.

Sundh, I., Mikkelä, C., Nilsson, M. and Svensson, B. H.: Potential aerobic methane oxidation in a Sphagnum-dominated peatland—Controlling factors and relation to methane emission, Soil Biol. Biochem., 27(6), 829–837, doi:https://doi.org/10.1016/0038-0717(94)00222-M, 1995.

Tarnocai, C.: The Impact of Climate Change on Canadian Peatlands, Can. Water Resour. J. / Rev. Can. des ressources hydriques, 34(4), 453–466, doi:10.4296/cwrj3404453, 2009.

Thompson, R. L., Sasakawa, M., Machida, T., Aalto, T., Worthy, D., Lavric, J. V, Lund Myhre, C. and Stohl, A.: Methane fluxes in the high northern latitudes for 2005–2013 estimated using a Bayesian atmospheric inversion, Atmos. Chem. Phys., 17(5), 3553–3572, doi:10.5194/acp-17-3553-2017, 2017.

Thonat, T., Saunois, M., Bousquet, P., Pison, I., Tan, Z., Zhuang, Q., Crill, P. M., Thornton, B. F., Bastviken, D., Dlugokencky, E. J., Zimov, N., Laurila, T., Hatakka, J., Hermansen, O. and Worthy, D. E. J.: Detectability of Arctic methane sources at six

sites performing continuous atmospheric measurements, Atmos. Chem. Phys., 17(13), 8371–8394, doi:10.5194/acp-17-8371-2017, 2017.

Tramontana, G., Jung, M., Schwalm, C. R., Ichii, K., Camps-Valls, G., Ráduly, B., Reichstein, M., Arain, M. A., Cescatti, A., Kiely, G., Merbold, L., Serrano-Ortiz, P., Sickert, S., Wolf, S. and Papale, D.: Predicting carbon dioxide and energy fluxes across global FLUXNET sites with regression algorithms, Biogeosciences, 13(14), 4291–4313, doi:10.5194/bg-13-4291-2016, 2016.

Treat, C. C., Bloom, A. A. and Marushchak, M. E.: Nongrowing season methane emissions–a significant component of annual emissions across northern ecosystems, Glob. Chang. Biol., 24(8), 3331–3343, doi:10.1111/gcb.14137, 2018.

Turetsky, M. R., Kotowska, A., Bubier, J., Dise, N. B., Crill, P., Hornibrook, E. R. C., Minkkinen, K., Moore, T. R., Myers-Smith, I. H., Nykänen, H., Olefeldt, D., Rinne, J., Saarnio, S., Shurpali, N., Tuittila, E.-S., Waddington, J. M., White, J. R., Wickland, K. P. and Wilmking, M.: A synthesis of methane emissions from 71 northern, temperate, and subtropical wetlands, Glob. Chang. Biol., 20(7), 2183–2197, doi:10.1111/gcb.12580, 2014.

Vermote, E.: MOD09A1 MODIS/Terra Surface Reflectance 8-Day L3 Global 500m SIN Grid V006. NASA EOSDIS LP DAAC. doi: 10.5067/MODIS/MOD09A1.006, 2015.

Waddington, J. M., Roulet, N. T. and Swanson, R. V: Water table control of CH_4 emission enhancement by vascular plants in boreal peatlands, J. Geophys. Res. Atmos., 101(D17), 22775–22785, doi:10.1029/96JD02014, 1996.

Wan, Z., Hook, S. and Hulley, G.: MOD11A2 MODIS/Terra Land Surface Temperature/Emissivity 8-Day L3 Global 1km SIN Grid V006. NASA EOSDIS LP DAAC. doi: 10.5067/MODIS/MOD11A2.006, 2015a.

Wan, Z., Hook, S. and Hulley, G.: MOD11C3 MODIS/Terra Land Surface Temperature/Emissivity Monthly L3 Global 0.05Deg CMG V006. NASA EOSDIS LP DAAC. doi: 10.5067/MODIS/MOD11C3.006, 2015b.

Wania, R., Ross, I. and Prentice, I. C.: Implementation and evaluation of a new methane model within a dynamic global vegetation model: LPJ-WHyMe v1.3.1, Geosci. Model Dev., 3(2), 565–584, doi:10.5194/gmd-3-565-2010, 2010.

Warwick, N. J., Cain, M. L., Fisher, R., France, J. L., Lowry, D., Michel, S. E., Nisbet, E. G., Vaughn, B. H., White, J. W. C. and Pyle, J. A.: Using δ13C-CH_4 and δD-CH_4 to constrain Arctic methane emissions, Atmos. Chem. Phys., 16(23), 14891–14908, doi:10.5194/acp-16-14891-2016, 2016.

Watts, J. D., Kimball, J. S., Bartsch, A. and McDonald, K. C.: Surface water inundation in the boreal-Arctic: potential impacts on regional methane emissions, Environ. Res. Lett., 9(7), doi:10.1088/1748-9326/9/7/075001, 2014.

Weedon, G. P., Balsamo, G., Bellouin, N., Gomes, S., Best, M. J. and Viterbo, P.: The WFDEI meteorological forcing data set: WATCH Forcing Data methodology applied to ERA-Interim reanalysis data, Water Resour. Res., 50(9), 7505–7514, doi:10.1002/2014WR015638, 2014.

Whalen, S. C.: Biogeochemistry of methane exchange between natural wetlands and the atmosphere, Environ. Eng. Sci., 22(1), 73–94, doi:10.1089/ees.2005.22.73, 2005.

Whiting, G. J. and Chanton, J. P.: Plant-dependent CH_4 emission in a subarctic Canadian fen, Global Biogeochem. Cycles, 6(3), 225–231, doi:10.1029/92GB00710, 1992.

Whiting, G. J. and Chanton, J. P.: Primary production control of methane emission from wetlands, Nature, 364(6440), 794–795 [online] Available from: http://dx.doi.org/10.1038/364794a0, 1993.

Wu, Z., Ahlstrom, A., Smith, B., Ardo, J., Eklundh, L., Fensholt, R. and Lehsten, V.: Climate data induced uncertainty in model-based estimations of terrestrial primary productivity, Environ. Res. Lett., 12(6), doi:10.1088/1748-9326/aa6fd8, 2017.

Xu, J., Morris, P. J., Liu, J. and Holden, J.: PEATMAP: Refining estimates of global peatland distribution based on a meta-analysis, CATENA, 160, 134–140, doi:https://doi.org/10.1016/j.catena.2017.09.010, 2018.

Xu, X., Riley, W. J., Koven, C. D., Billesbach, D. P., Chang, R. Y.-W., Commane, R., Euskirchen, E. S., Hartery, S., Harazono, Y., Iwata, H., McDonald, K. C., Miller, C. E., Oechel, W. C., Poulter, B., Raz-Yaseef, N., Sweeney, C., Torn, M., Wofsy, S. C., Zhang, Z. and Zona, D.: A multi-scale comparison of modeled and observed seasonal methane emissions in northern wetlands, Biogeosciences, 13(17), 5043–5056, doi:10.5194/bg-13-5043-2016, 2016a.

Xu, X., Yuan, F., Hanson, P. J., Wullschleger, S. D., Thornton, P. E., Riley, W. J., Song, X., Graham, D. E., Song, C. and Tian, H.: Reviews and syntheses: Four decades of modeling methane cycling in terrestrial ecosystems, Biogeosciences, 13(12), 3735–3755, doi:10.5194/bg-13-3735-2016, 2016b.

Yvon-Durocher, G., Allen, A. P., Bastviken, D., Conrad, R., Gudasz, C., St-Pierre, A., Thanh-Duc, N. and del Giorgio, P. A.: Methane fluxes show consistent temperature dependence across microbial to ecosystem scales, Nature, 507(7493), 488–+, doi:10.1038/nature13164, 2014.

Zarco-Tejada, P. J. and Ustin, S. L.: Modeling canopy water content for carbon estimates from MODIS data at land EOS validation sites, in IGARSS 2001. Scanning the Present and Resolving the Future. Proceedings. IEEE 2001 International Geoscience and Remote Sensing Symposium (Cat. No.01CH37217), vol. 1, pp. 342–344 vol.1., 2001.

Zhang, Y., Xiao, X., Wu, X., Zhou, S., Zhang, G., Qin, Y. and Dong, J.: A global moderate resolution dataset of gross primary production of vegetation for 2000–2016, Sci. Data, 4, 170165 [online] Available from: http://dx.doi.org/10.1038/sdata.2017.165, 2017a.

Zhang, Z., Zimmermann, N. E., Kaplan, J. O. and Poulter, B.: Modeling spatiotemporal dynamics of global wetlands: comprehensive evaluation of a new sub-grid TOPMODEL parameterization and uncertainties, Biogeosciences, 13(5), 1387–1408, doi:10.5194/bg-13-1387-2016, 2016.

Zhang, Z., Zimmermann, N. E., Stenke, A., Li, X., Hodson, E. L., Zhu, G., Huang, C. and Poulter, B.: Emerging role of wetland methane emissions in driving 21st century climate change, Proc. Natl. Acad. Sci. [online] Available from: http://www.pnas.org/content/early/2017/08/16/1618765114.abstract, 2017b.

Zhao, J., Peichl, M. and Nilsson, M. B.: Enhanced winter soil frost reduces methane emission during the subsequent growing season in a boreal peatland, Glob. Chang. Biol., 22(2), 750–762, doi:10.1111/gcb.13119, 2016.

Zhao, M., Heinsch, F. A., Nemani, R. R. and Running, S. W.: Improvements of the MODIS terrestrial gross and net primary production global data set, Remote Sens. Environ., 95(2), 164–176, doi:https://doi.org/10.1016/j.rse.2004.12.011, 2005.

Zhu, Q., Liu, J., Peng, C., Chen, H., Fang, X., Jiang, H., Yang, G., Zhu, D., Wang, W. and Zhou, X.: Modelling methane emissions from natural wetlands by development and application of the TRIPLEX-GHG model, Geosci. Model Dev., 7(3), 981–999, doi:10.5194/gmd-7-981-2014, 2014.

Zhu, X., Zhuang, Q., Qin, Z., Glagolev, M. and Song, L.: Estimating wetland methane emissions from the northern high latitudes from 1990 to 2009 using artificial neural networks, Global Biogeochem. Cycles, 27(2), 592–604, doi:10.1002/gbc.20052, 2013.

Zona, D., Oechel, W. C., Kochendorfer, J., Paw U, K. T., Salyuk, A. N., Olivas, P. C., Oberbauer, S. F. and Lipson, D. A.: Methane fluxes during the initiation of a large-scale water table manipulation experiment in the Alaskan Arctic tundra, Global Biogeochem. Cycles, 23(2), doi:10.1029/2009GB003487, 2009.

Zona, D., Gioli, B., Commane, R., Lindaas, J., Wofsy, S. C., Miller, C. E., Dinardo, S. J., Dengel, S., Sweeney, C., Karion, A., Chang, R. Y.-W., Henderson, J. M., Murphy, P. C., Goodrich, J. P., Moreaux, V., Liljedahl, A., Watts, J. D., Kimball, J. S., Lipson, D. A. and Oechel, W. C.: Cold season emissions dominate the Arctic tundra methane budget, Proc. Natl. Acad. Sci., 113(1), 40 LP-45 [online] Available from: http://www.pnas.org/content/113/1/40.abstract, 2016.

Zürcher, S., Spahni, R., Joos, F., Steinacher, M. and Fischer, H.: Impact of an abrupt cooling event on interglacial methane emissions in northern peatlands, Biogeosciences, 10(3), 1963–1981, doi:10.5194/bg-10-1963-2013, 2013.

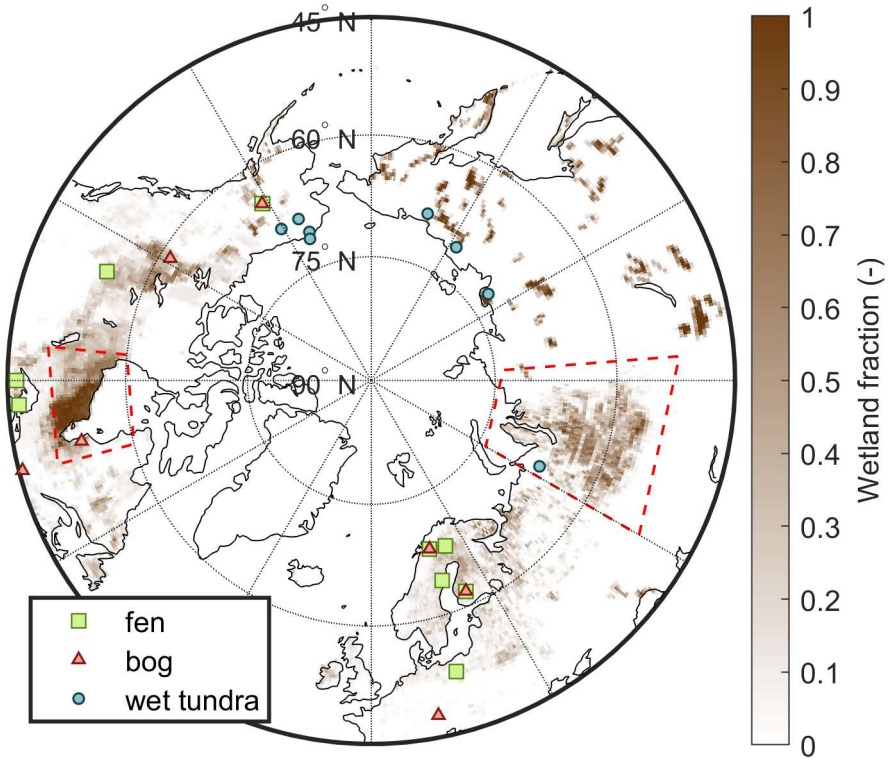

Figure 1: Map showing the locations of the EC measurements. The distribution of wetlands shown in the figure is based on Xu et al. (2018). Hudson Bay Lowlands (50°N-60°N, 75°W-96°W) and Western Siberian Lowlands (52°N-74°N, 60°E-94.5°E) are highlighted with red dashed lines.

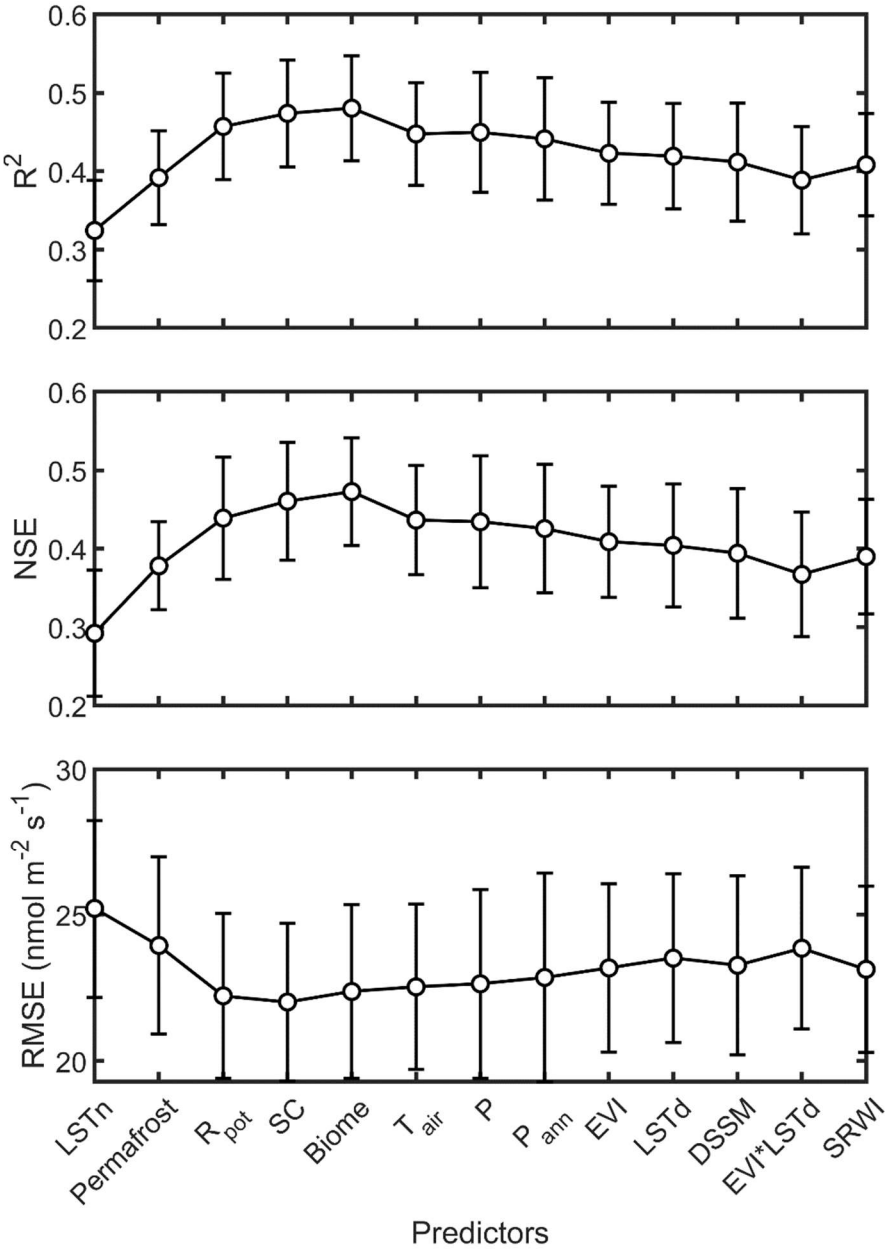

Figure 2. Evolution of statistical metrics during RF model development. Predictors were added to the RF model starting from the left of the figure and accumulate along the x-axis. For instance, the x-tick label "SC" shows the RF model performance when LSTn, Permafrost, Rpot, and SC were used as predictors in the model. See the x-tick label explanations in Table 1. The error bars denote 1-sigma uncertainty of the values estimated with bootstrapping.

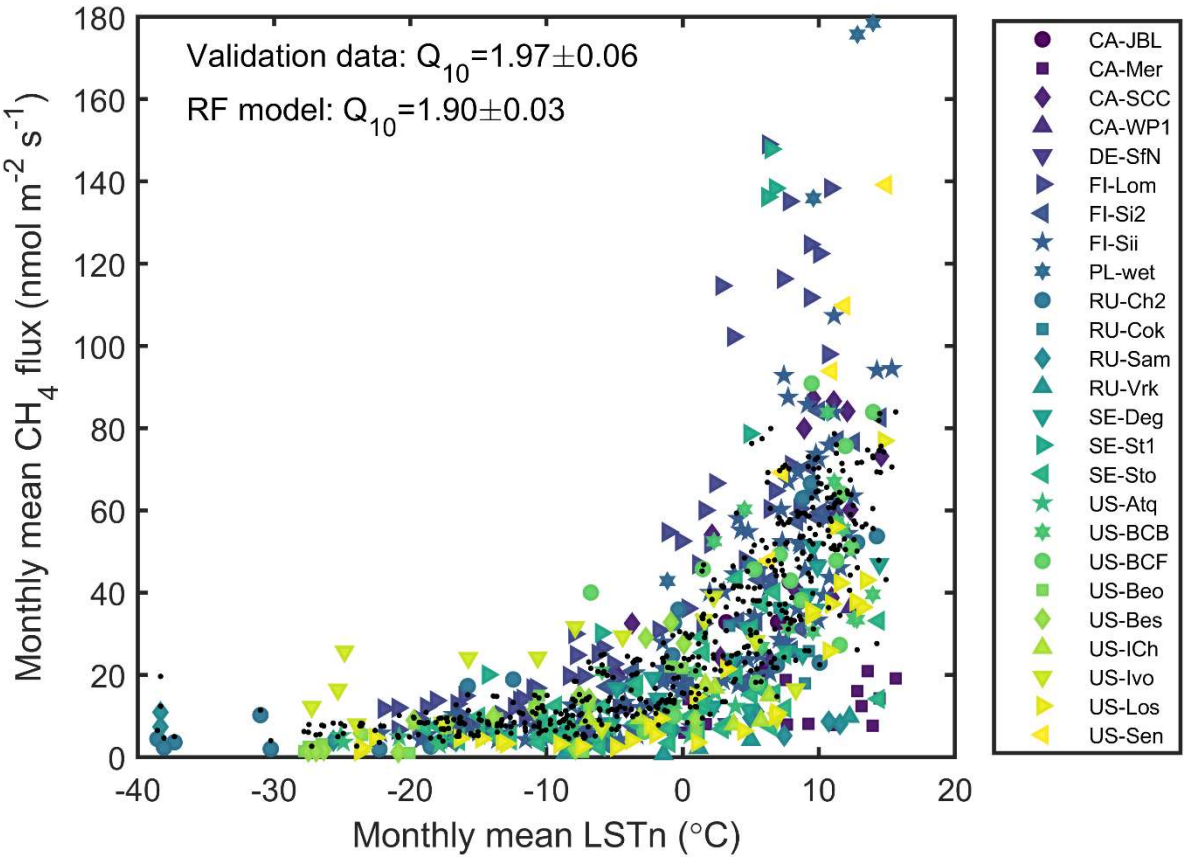

Figure 3. Dependence of monthly mean CH_4 emissions on monthly mean land surface temperature at night (LSTn) derived from MODIS data. Eddy covariance measurements are shown with filled markers (unique colour for each site) and random forets model predictions for each site are given with black dots.

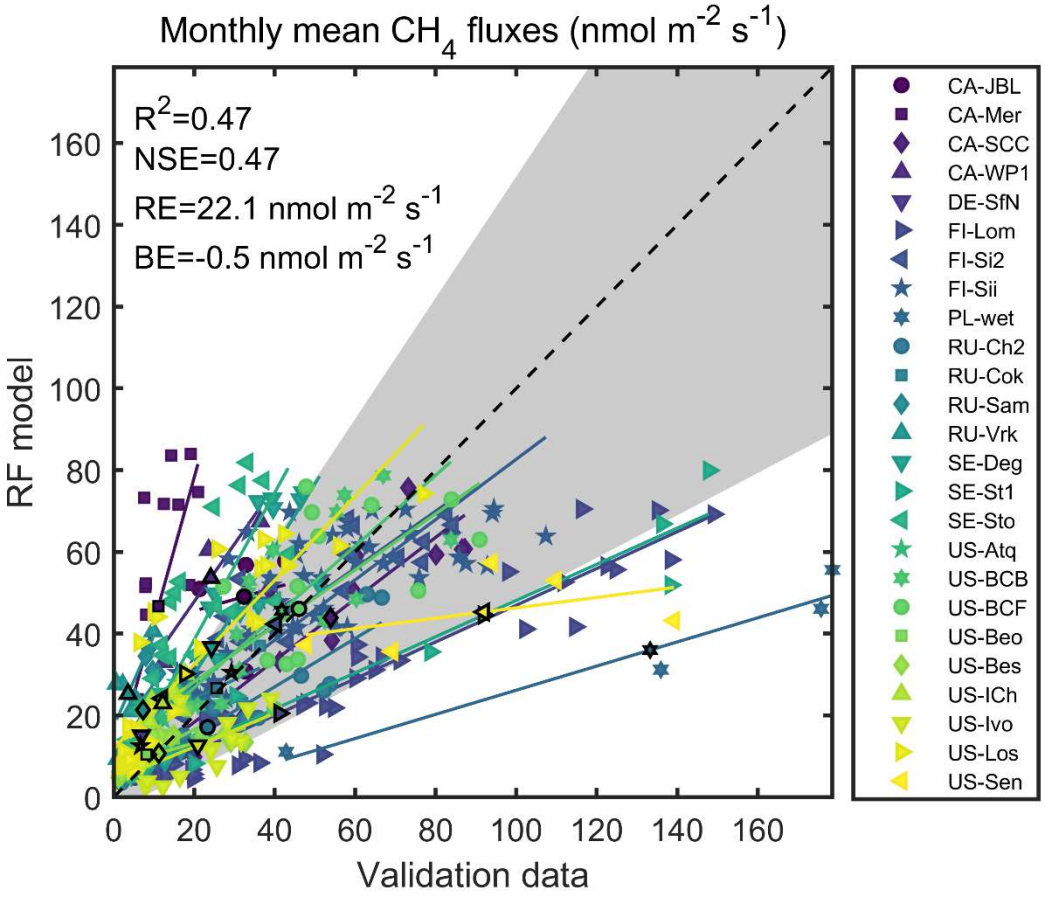

Figure 4. Relation between monthly mean CH_4 fluxes predicted by the RF model and independent validation data. Monthly average values from the same site are identified by unique colours and least squares linear fit to data from each site is also plotted using the same colour. Site means are shown with markers with black edges. The dashed line shows the 1:1 line. The shaded area shows the uncertainty range estimated from the RE CH_4 flux dependence (see text for further details). The statistics in the figure are calculated using the monthly data.

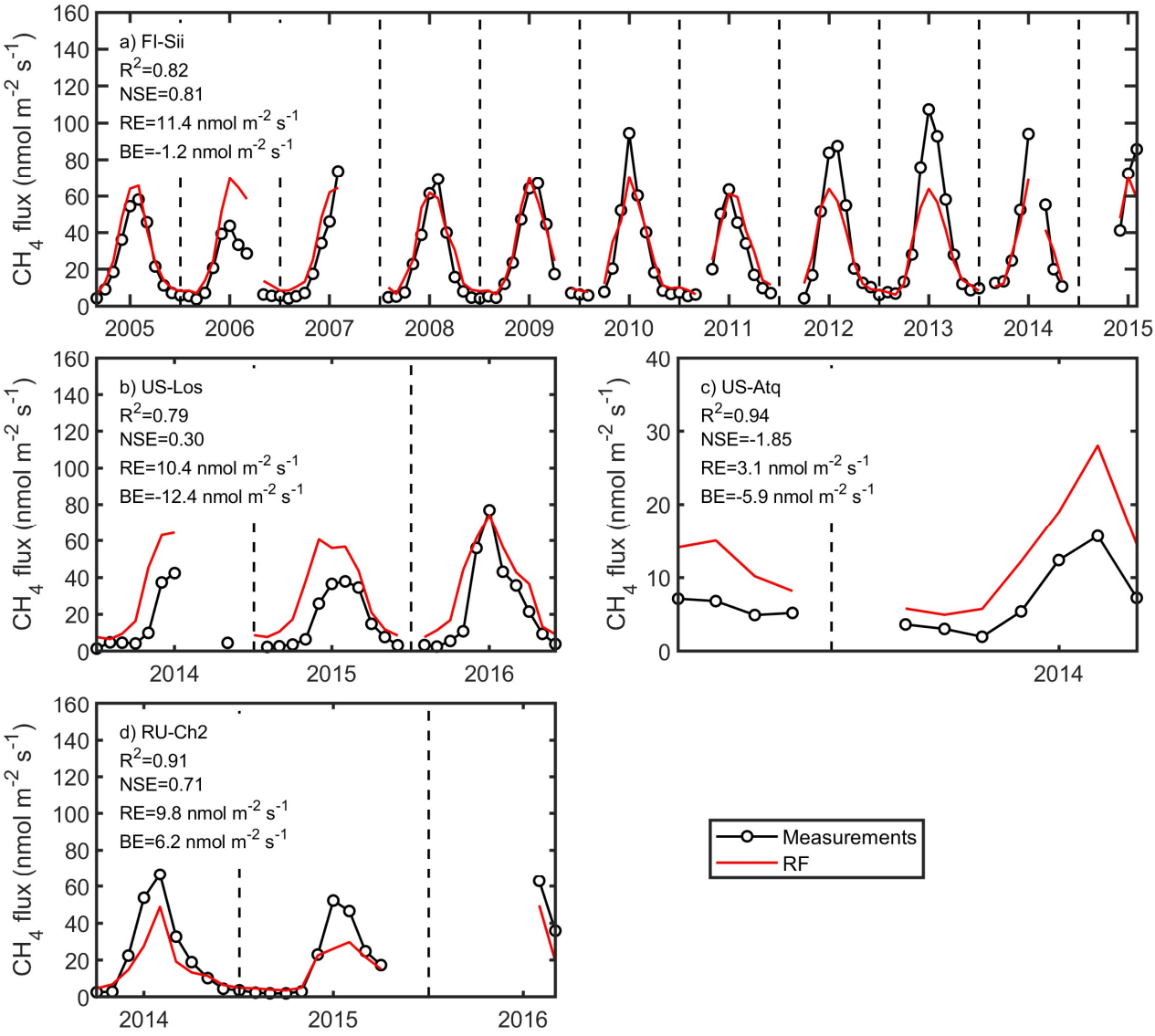

Figure 5. Time series of modelled CH_4 emissions (red lines) together with validation data (circles) at four example sites: a) Siikaneva oligotrophic fen in Finland, b) Lost Creek shrub fen in Wisconsin, US, c) Atqasuk wet tundra in Alaska, US and d) Chersky wet tundra in northeast Siberia, Russia. Vertical dashed lines denote a new year. Note the changes in y-axis scales. Site specific model performance metrics are also included.

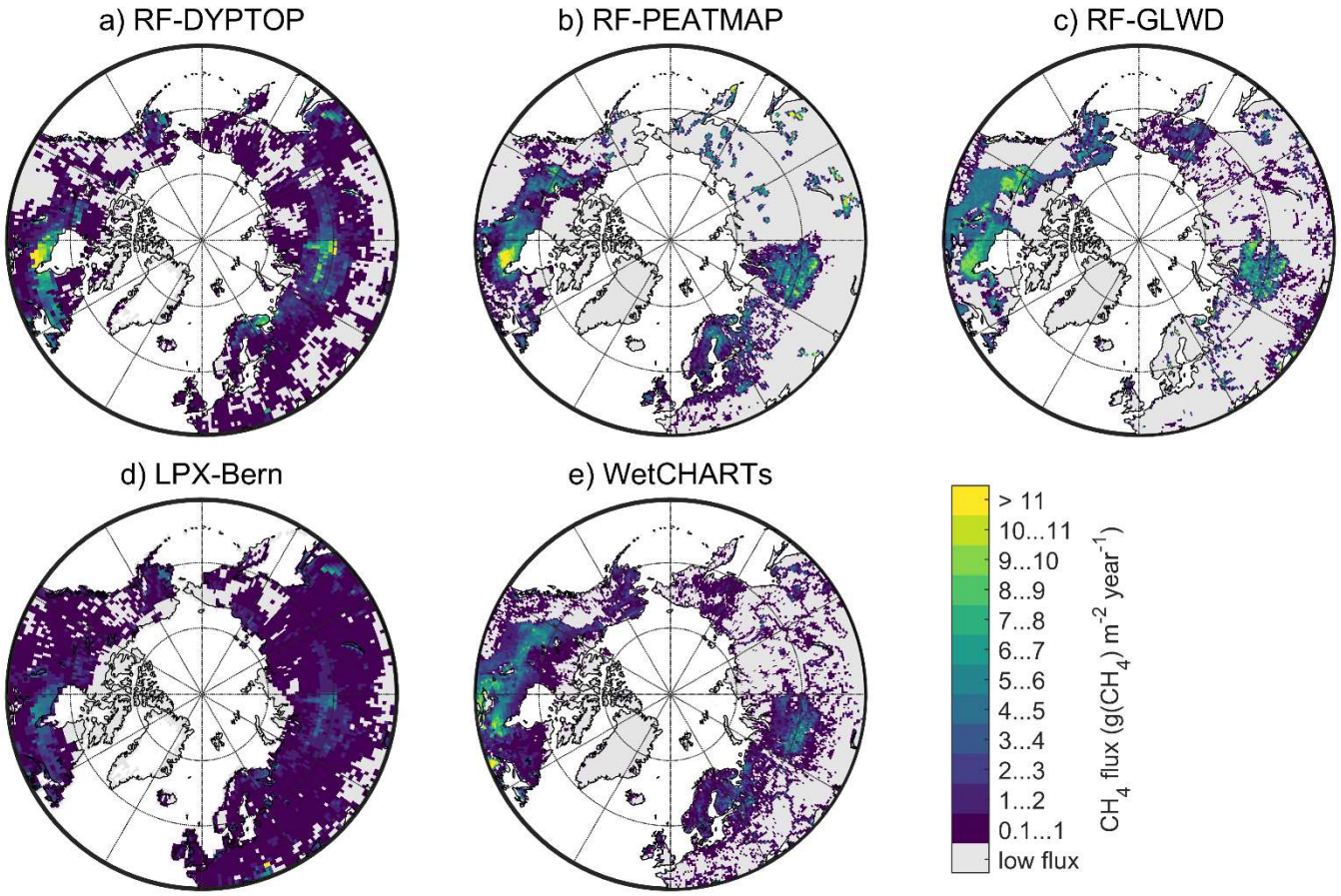

Figure 6. Mean annual CH_4 wetland emissions during years 2013-2014 estimated by upscaling EC data using the RF model and three wetland maps (top row) and process models (bottom row). Grid cells with low CH_4 wetland emissions (below 0.1 g(CH_4) m^{-2} $year^{-1}$) are shown with grey. The flux rates refer to total unit area in a grid cell.

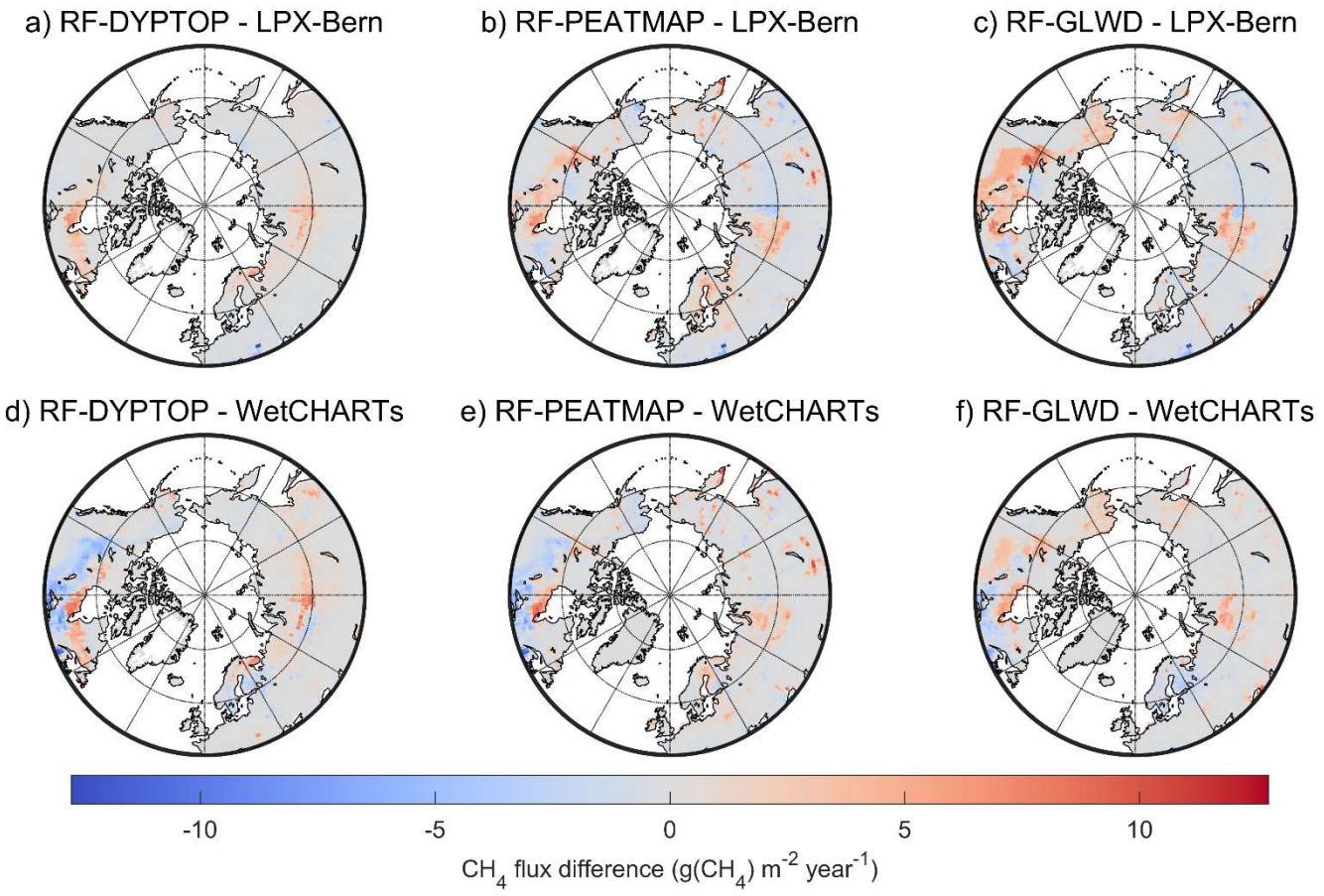

Figure 7. Difference in mean annual CH_4 wetland emissions during years 2013-2014 estimated by upscaling EC data using the RF model with different wetland maps and process models. All the CH_4 emission maps were aggregated to 1° resolution before comparison. The flux rates refer to total unit area in a grid cell.

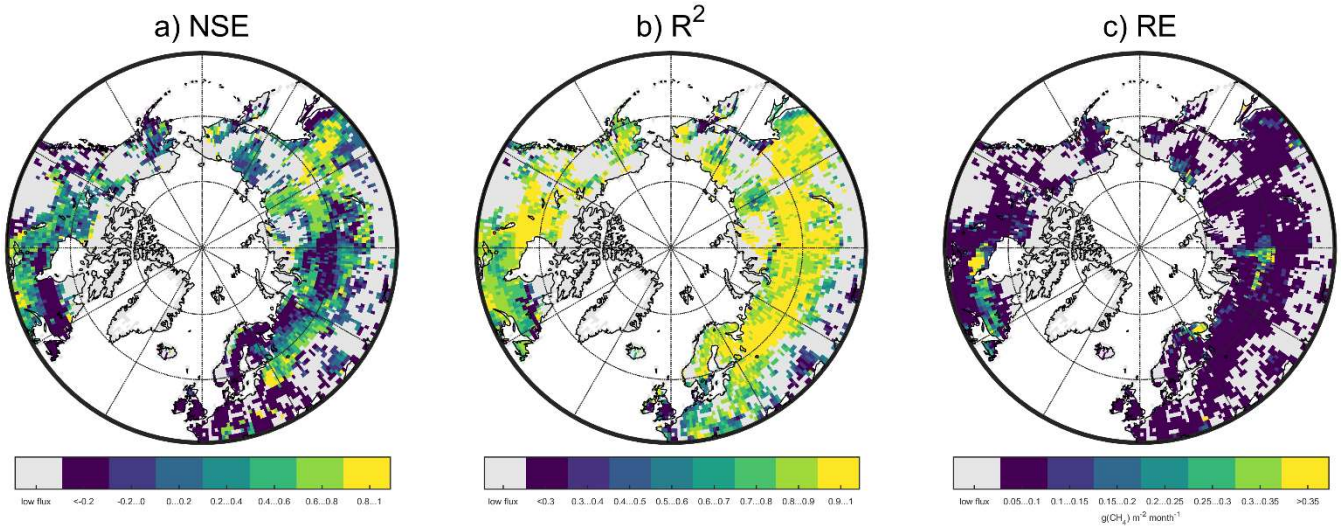

Figure 8. NSE, R^2 and RE calculated between RF-DYPTOP and LPX-Bern. Grid cells with low CH_4 wetland emissions (below 0.1 g(CH_4) m^{-2} $year^{-1}$) are shown with grey. RE values refer to total unit area in a grid cell.

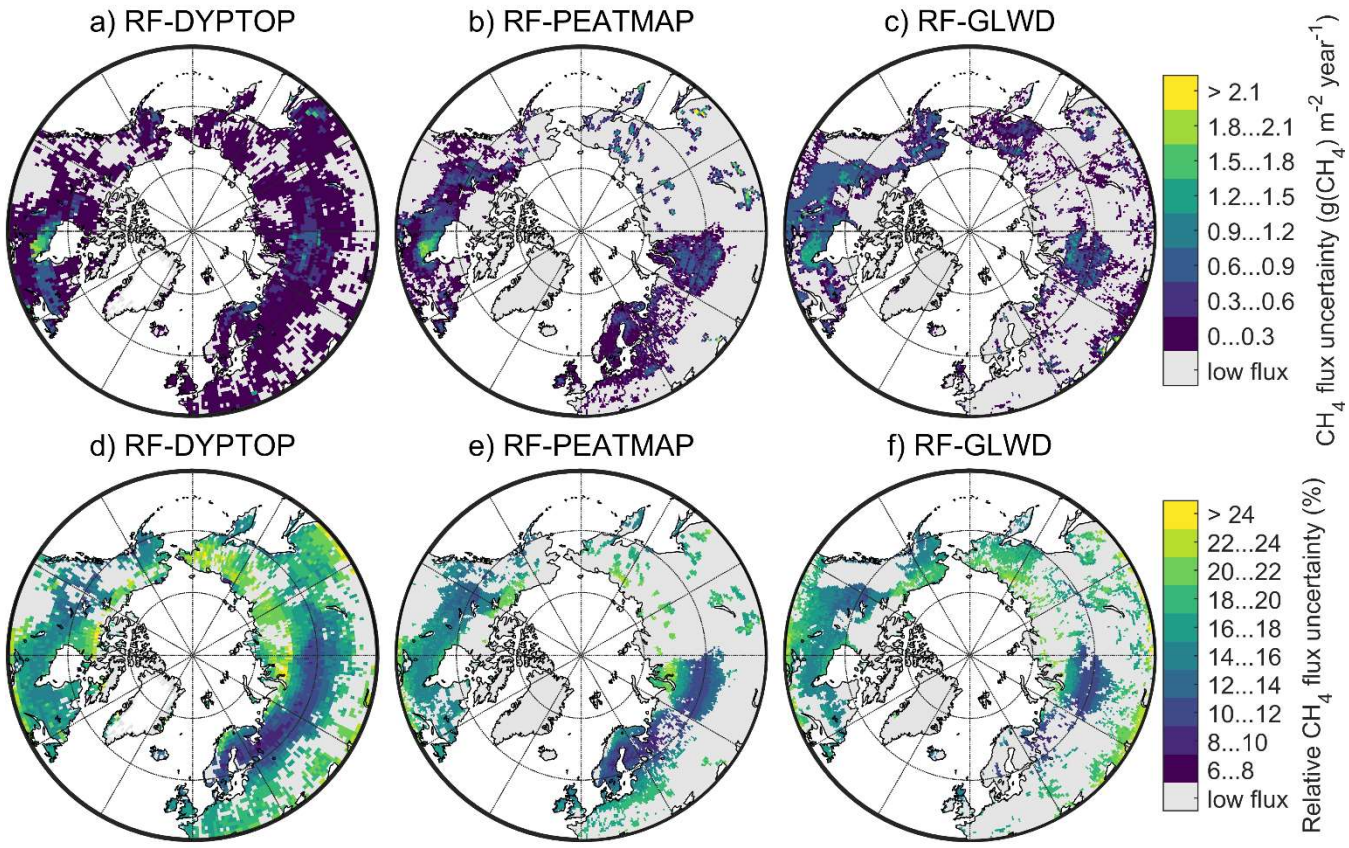

Figure 9. Absolute (subplots a)-c)) and relative (subplots d)-f)) uncertainties of the upscaled CH_4 fluxes using different wetland maps. Uncertainty is estimated as 1-σ variability of the predictions by 200 RF models developed by bootstrapping the training data (Sect. 2.1.2). Grid cells with low CH_4 wetland emissions (below 0.1 g(CH_4) m^{-2} $year^{-1}$) are shown with grey. The absolute uncertainties refer to total unit area in a grid cell.

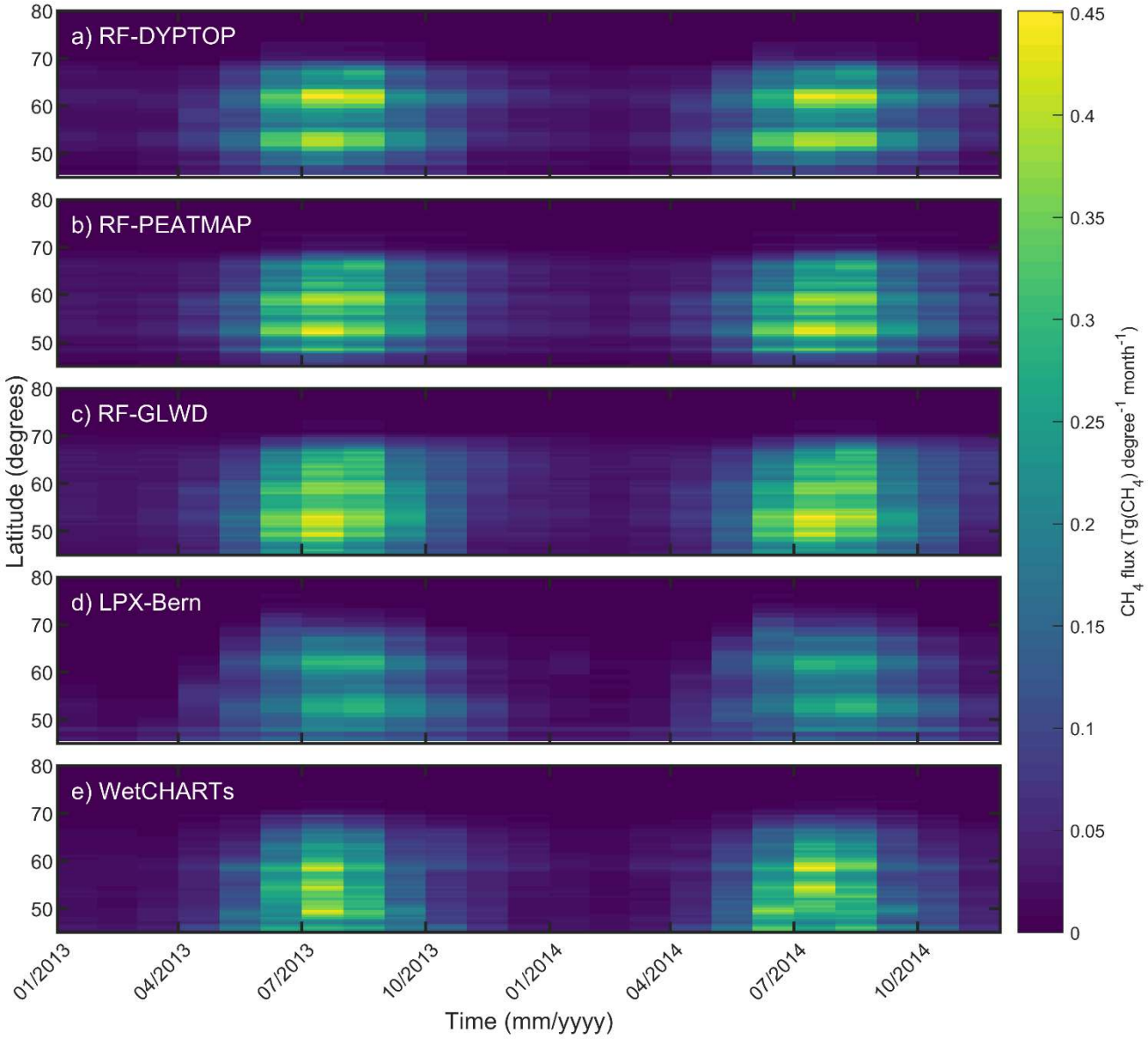

Figure 10. Monthly time series of zonal mean CH_4 fluxes. The upscaled fluxes with different wetland maps are shown in subplots a), b) and c) and wetland CH_4 emissions estimated with the two process models are given in subplots d) and e).

Table 1. Description of input variables for RF model development for upscaling. Data were aggregated to monthly values (see text) unless otherwise noted below.

	Name	Description	Data source	Available in gridded format
Site measurements	T_{air}	Mean air temperature	site PI & WFDEI	Yes
	P	Precipitation	site PI & WFDEI	Yes
	P_{ann}	Annual precipitation	site PI & WFDEI	Yes
Remote sensing	LSTn	Land surface temperature at night	MOD11A2	Yes
	LSTd	Land surface temperature at day	MOD11A2	Yes
	EVI	Enhanced vegetation index	MOD13A3	Yes
	SRWI	Simple ratio water index (SRWI = R_{858}/R_{1240})	MOD09A1	Yes
	SC	Snow cover flag	MOD10A1	Yes
	EVI* LSTd	Product of EVI and LSTd, a proxy for GPP (Schubert et al., 2010)	MOD13A3 & MOD11A2	Yes
Additional categorical variables	Permafrost	Flag for permafrost at site (true/false)	site PI	Yes
	Biome	Site classification based on biome (temperate, boreal and tundra)	Olson et al. (2001)	Yes
	type	Wetland type (fen, bog, tundra)	site PI	No
	sedge	flag for sedges as dominant vegetation type (true/false)	site PI	No
Other	R_{pot} & der(R_{pot})	Potential solar radiation at the top of atmosphere and its first time derivative	-	Yes
	DSSM	Days since snowmelt, derived from the snow cover flag	-	Yes

Table 2. Annual CH_4 wetland emissions in different subdomains (Hudson Bay lowlands and Western Siberian lowlands, see Fig. 1) and time periods. The values are given in Tg(CH_4) year^{-1}. Note that estimates from some reference studies are not for the same period as the one studied here (2013-2014). For WetCHARTs the mean of the model ensemble together with the range (in parentheses) are given, whereas for the upscaling results the 95 % confidence intervals for the estimated emissions are given.

	Reference	Hudson Bay lowlands	Western Siberian lowlands	Nongrowing season fluxes from northern wetlands (November…March)	Annual emissions north from 45 °N
Inversion models	Bohn et al. (2015), WETCHIMP-WSL		6.06 ± 1.22		
	Bruhwiler et al. (2014)[a]				23
	Kim et al. (2011)		2.9 ± 1.7 and 3.0 ± 1.4		
	Miller et al. (2014)	2.4 ± 0.3			
	Spahni et al. (2011)				28.2 ± 2.2
	Thompson et al. (2017)	2.7-3.4	6.9 ± 3.6		
Process models	Bohn et al. (2015), WETCHIMP-WSL		5.34 ± 0.54		
	Chen et al. (2015)[b]	3.11 ± 0.45			35.0 ± 6.7
	Melton et al. (2013), WETCHIMP[c]	5.4 ± 3.2			
	Pickett-Heaps et al. (2011)[d]	2.3 ± 0.3			
	Treat et al. (2018)[e]			6.1 ± 1.5	37 ± 7
	Watts et al. (2014)				53
	Zhang et al. (2016)[f]	5.5 ± 1.1	4.6 ± 0.6		30.3± 5.4
	This study, LPX-Bern	2.5	4.4	4.5	24.7
	This study, WetCHARTs	2.8 (0.5-8.7)	4.2 (1.6-9.4)	5.1 (0.6-17.0)	29.7 (8.7-74.0)
Flux measurement upscaling	Glagolev et al. (2011)		3.9 ± 1.3		
	Zhu et al. (2013)				44.0-53.7
	This study, RF-PEATMAP	4.8 (3.3-6.3)	6.6 (4.9-8.4)	6.7 (4.9-8.5)	31.7 (22.3-41.2)

	This study, RF-DYPTOP	4.6 (3.1-6.0)	7.0 (5.2-8.8)	6.2 (4.6-7.8)	30.6 (21.4-39.9)
	This study, RF-GLWD	4.9 (3.4-6.5)	6.8 (5.0-8.5)	8.0 (5.8-10.2)	37.6 (25.9-49.5)

a Approximately north from 47 °N

b Approximately north from 45 °N

c Mean annual CH_4 emissions from eight models ± 1-sigma of interannual variation in the model estimates for the period 1993-2004.

d Process model tuned to match atmospheric observations

e North from 40 °N

f Mean ± 1-sigma over LPJ-wsl model results using different wetland extends for the period 1980-2000.